AD NUMBER

AD479489

NEW LIMITATION CHANGE

TO

Approved for public release, distribution unlimited

FROM

Distribution: Further dissemination only as directed by Office of Naval Research, Arlington VA 22217-0000; Sep 1965 or higher DoD authority.

AUTHORITY

ONR ltr 27 Jul 1971

HYDRODYNAMICS LABORATORY

KÁRMÁN LABORATORY OF FLUID MECHANICS AND JET PROPULSION

CALIFORNIA INSTITUTE OF TECHNOLOGY

PASADENA, CALIFORNIA

Hydrodynamics Laboratory
Kármán Laboratory of Fluid Mechanics and Jet Propulsion
California Institute of Technology
Pasadena, California

EVALUATION OF PRESSURE DISTRIBUTION ON A CAVITATING HYDROFOIL WITH FLAP

by

Zora L. Harrison
and
Duen-pao Wang

This work was carried out under the
Bureau of Ships General Hydrodynamics Research Program,
Administered by the David Taylor Model Basin,
Office of Naval Research Contract Nonr-220(52).

Report No. E-133.1 September 1965

ABSTRACT

A general method is established to calculate the pressure distribution and the moment of force for a two-dimensional, supercavitating hydrofoil with a flap. The wake flow model is adopted to describe the configuration of the flow field. Some numerical results for a supercavitating flat plate with a flap are compared with the corresponding experimental data.

NOMENCLATURE

A	a scale factor
a_1, a_2	distances from the hinge point, P, to the respective centers of pressure of the main body and the flap
AR	aspect ratio
c_1, c_2	distances along the chord, measured from the hinge point
C_D	total drag coefficient
C_{F_1}, C_{F_2}	total normal force coefficients acting at the centers of pressure
C_L	total lift coefficient
C_{M_1}, C_{M_2}	moment coefficients about the hinge point
C_{M_H}	moment coefficient of the flap about the hinge point, $C_{M_H} = C_{M_2}$
$C_{M_{LE}}$	total moment coefficient about the leading edge
C_p, C'_p	pressure coefficients
C_{x_1}, C_{x_2}	force components in x-direction
C_{y_1}, C_{y_2}	force components in y-direction
$f(t)$	complex potential
f/c	flap to chord ratio
$g(t;t_o)$	an analytic function: $g(t; t_o) = \frac{1}{2A\zeta} \frac{df(t)}{dt}$
H	function in the integrand of β_a
h/c	the ratio of the depth of submergence to the chord length
I_1, I_2	integrals in the calculation of ℓ_1 and ℓ_2
J_1, J_2	Cauchy integrals in the calculation of chord length

ℓ_1, ℓ_2	chord lengths: $\ell_1 + \ell_2 = 1$, $f/c = \ell_2 / (\ell_1 + \ell_2)$
Q	function in the integrand of V_a
r_1, r_2	distance parameters in the calculation of V_f and β_f (note the subscripts 1 and 2 do not refer to the main body and the flap for these parameters)
R	the prescribed value of f/c
$s(x)$	chord distance measured from the leading edge
t	a mapping plane of the flow region
t_o	image point of $z = \infty$ in the t-plane: $t_o = Ve^{-i\beta}$
T	image of the hinge point in the t-plane
U	free stream velocity: $U^{-2} = 1 + \sigma$
V	magnitude of t_o
w(t)	complex velocity
x	coordinate in z-plane and transformation variable
y	coordinate in z-plane
z	physical plane
α	angle of attack
β	polar angle of t_o in the t-plane
$\epsilon\pi$	flap angle
θ_1, θ_2	angles between the tangents to the foil profile and the chords
σ	cavitation number
τ	integration variable in the t-plane

Introduction

In practical applications of supercavitating hydrofoils the adoption of flaps or other load modulators as motion control devices is of fundamental importance. An accurate determination of the moment and hinge-moment acting on supercavitating hydrofoils with deflected flaps is essential to the structure design on one hand, and to the development of successful control and maneuvability on the other. Furthermore, a detailed study of the pressure distribution is also valuable for establishing the general validity of any theoretical model and also for elucidating the role of effectiveness of the flap.

Recently, the supercavitating flap problem has been investigated using the linearized theory for the case of zero cavitation number, corresponding to an infinitely long cavity. The case of infinite flow extent was first treated by Tulin and Burkart [1][1]. This theory has been extended by Johnson [2] who incorporated the classical work of Kirchhoff and Rayleigh, and that of Green, the latter including the effect of the free water surface, but neglecting the gravity effect. In Johnson's theory, an estimate of the effect of finite aspect ratio is also evaluated. A linearized theory was subsequently developed by Auslaender [3] for the case of zero cavitation number and at a finite depth of submergence. Using a nonlinear theory, Lin [4] treated the flap problem for the flat plate hydrofoil at zero cavitation number. In an approximate sense, the limiting condition of zero cavitation number corresponds to the shallow submergence case when the

[1] Numbers in brackets designate references at end of paper.

cavity becomes completely open to the atmosphere. However, a fine difference in this correspondence arises from the fact that the dynamic effect due to the upper half flow field is actually modified in the presence of a free water surface at shallow submergences. In accordance with this analogous configuration, some model investigations with flaps have been carried out by Johnson [2], Brown [5], Conolly [6] and Wetzel and Maxwell [7]. In order to establish the fully cavitating configuration at small incidences, the technique of base ventilation has been employed in some cases of these experiments.

The objective of the present investigation is to establish a general and systematic method for calculating accurately the pressure distribution, moment of force, and hinge-moment acting on a supercavitating hydrofoil of arbitrary profile, especially when the angle of attack, flap deflection and the cavitation number are moderate or large. This calculation is based on the nonlinear theory developed recently by Wu and Wang [8]. To meet the general operating conditions in practice, this theory can be further extended to include the effects of free water surface and gravity, and finally the effect of finite aspect ratio and three-dimensional features. The scope of the present work, however, will be limited to the case of two-dimensional flow of infinite extent, with emphasis on the pressure distribution over a flapped hydrofoil. The formulas for the force moment and hinge-moment are also derived here. Since the information about pressure distribution in cavity flows is relatively scarce in the existing literature, it is hoped that the results of this study may provide useful data for future applications as well as for further development of this general field.

The numerical computation has been performed with an IBM 7094 Computer, for which the method and computing program are explained in detail in this report. The final results for the case of flat plate hydrofoil with a flap are presented in figures for different angles of attack, flap angles, flap-chord ratio and the cavitation number. The calculation for hydrofoils of arbitrary profile is also discussed. The computation program for this case follows an approximate numerical scheme developed by Wu and Wang [9]. This approximate method greatly shortens the computation of the final integral equations in the theory, while still retaining a high degree of accuracy of the result.

A parallel experimental program has been accomplished by Meijer, the results of these experiments will be presented in a separate report by Meijer [10]. It can be stated here that the general agreement between the theory and experiments is very satisfactory, and the experimental observation has also revealed some interesting points, such as the viscous effect near the flap hinge. With the theory now well established in the typical cases so far investigated, the present method can be applied with confidence for the general case of arbitrary profile.

General Formulation

We consider a steady, irrotational plane flow of an incompressible fluid past an arbitrary profile AB in such a way that the flow is separated from the leading and trailing edges A and B, forming a fully developed cavity behind the foil AB. The foil AB consists of a main foil AP and a flap PB, as shown in Fig. 1(a). A set of Cartesian coordinates, x and

y, is chosen with the origin at the leading edge A and the x-axis lying along the chord AP. The incoming free stream has a speed U and is at an angle of attack α to the x-axis. The flap angle, $\epsilon\pi$, is the angle measured from the x-axis to the chord of the flap PB, positive in the clockwise sense.

In the following analysis the wake flow model, as formulated in [8], will be used to describe the flow. For the sake of convenience, a general description of the wake model will be given briefly in the following: The part AC and BC' of the free streamlines, as shown in Fig.1(a), form the boundary of a near-wake of constant pressure p_c, which is less than the free stream pressure p_∞. From this part onward the pressure varies continually and monotonically from p_c to p_∞, along the far-wake boundary, CI and C'I. It is further assumed that the values of the complex potential, f, and the complex velocity, w, at the point C are equal to those at the point C' respectively. With the introduction of the so-called "hodograph-slit condition" for the streamlines CI and C'I, we assume that the entire flow region in the z-plane can be mapped onto the interior of the lower-half unit circle in a t-plane, as shown in Fig. 1(b), where T is the image of the point P, and t_o that of the point I. On the t-plane the complex potential, f, and the complex velocity, w, with the speed on the cavity wall normalized to unity, can be written respectively as

$$f = \frac{A t^2}{(t - t_o)(t - \bar{t}_o)(t - \frac{1}{t_o})(t - \frac{1}{\bar{t}_o})}, \qquad (1a)$$

and

$$w = t\left|\frac{t-T}{Tt-1}\right|^{\epsilon}\left\{\exp\left[-\frac{(1-t^2)}{\pi}\int_{-1}^{1}\frac{\theta(z(\tau))\,d\tau}{(\tau-t)(\pi t-1)}\right]\right\}, \tag{1b}$$

where $\theta(z(\tau))$ is the angle measured from the chord AP (or, chord PB), counter-clockwise as positive, to the tangent at any point z on the surface profile curve AP (or, curve PB), as shown in Fig. 1(a). At $z=\infty$, $w = Ue^{-i\alpha}$ and $t = t_o$, hence

$$t_o = Ue^{-i\alpha}\left(\frac{Tt_o-1}{t_o-T}\right)^{\epsilon}\left\{\exp\left[\frac{(1-t^2)}{\pi}\int_{-1}^{1}\frac{\theta(z(\tau))\,d\tau}{(\tau-t_o)(\pi t_o-1)}\right]\right\}. \tag{2}$$

For any point on the foil, corresponding to $t=\tau$, τ being real, $-1<\tau<1$, the distance along AP and PB between the leading edge A and the projection of this point to AP or PE is given by:

$$c(\tau) = 2A\int_{-1}^{\tau}\left|\frac{1-Tt}{T-t}\right|^{\epsilon} g(t;t_o)\left\{\exp\left[\frac{1-t^2}{\pi}\int_{-1}^{*1}\frac{\theta(z(\tau'))\,d\tau'}{(\tau'-t)(\tau't-1)}\right]\cos\theta(z(t))\right\}dt \tag{3}$$

where * above the integral sign signifies that the Cauchy principal value of the integral is taken and

$$g(t;t_o) = \frac{1}{2At}\frac{df}{dt} = \frac{(1-t^2)\left[1+t^2-\frac{1}{2}t(t_o+\bar{t}_o)(1+t_o^{-1}\bar{t}_o^{-1})\right]}{\left[(t-t_o)\,(t-\bar{t}_o)\,(t-t_o^{-1})\,(t-\bar{t}_o^{-1})\right]^2}. \tag{4}$$

The condition that the points C, C' lie on the lower unit circle in the t-plane, or $-\pi<\arg t_c<0$, may be expressed as

$$-1<\mathrm{Re}\,\tfrac{1}{2}(t_o+\frac{1}{t_o})<1.$$

This condition is equivalent to stating that the constant pressure region extends beyond the trailing edge B.

By writing $t_o = Ve^{-i\beta}$, Eq. (4) becomes

$$g(t; t_o) = \frac{V^4 (1 - t^2)[1 + t^2 - (1 + V^{-2})(tV \cos \beta)]}{[(t^2 + V^2 - 2tV \cos \beta)(t^2 V^2 - 2tV \cos \beta + 1)]^2} . \tag{5}$$

Similarly, substituting $t_o = Ve^{-i\beta}$ into Eq. (2), expanding and separating the real and imaginary parts, we obtain the parametric relations for t_o as follows

$$V = V_f V_a , \tag{6}$$

and

$$\beta = \beta_f + \beta_a , \tag{7}$$

where

$$V_f = U \left(\frac{T r_2}{r_1} \right)^{\epsilon} , \tag{8}$$

$$V_a = \exp \left[\frac{1}{\pi} \int_{-1}^{1} Q(t) \theta(t) \, dt \right] , \tag{9}$$

$$\beta_f = \alpha + \epsilon \left\{ \cos^{-1} \left[\frac{r_1^2 + r_2^2 - \left(\frac{1}{T} - T \right)^2}{2 r_1 r_2} \right] \right\} , \tag{10}$$

$$\beta_a = - \frac{1}{\pi} V \sin \beta \int_{-1}^{1} H(t) \theta(t) \, dt , \tag{11}$$

$$r_1 = (T^2 + V^2 - 2TV \cos \beta)^{\frac{1}{2}} , \tag{12}$$

$$r_2 = (T^{-2} + V^2 - 2T^{-1} V \cos \beta)^{\frac{1}{2}} , \tag{13}$$

$$Q(t) = \frac{tV^2 - V\cos\beta}{t^2V^2 - 2tV\cos\beta + 1} - \frac{t - V\cos\beta}{t^2 + V^2 - 2tV\cos\beta} \tag{14}$$

and

$$H(t) = \frac{1}{t^2V^2 - 2tV\cos\beta + 1} + \frac{1}{t^2 + V^2 - 2tV\cos\beta} . \tag{15}$$

Let J(t) denote the Cauchy integral in Eq. (3). Then, noting that

$$\int_{-1}^{*1} \frac{d\tau}{(\tau - t)(\tau t - 1)} = 0 ,$$

the singularity of the integrand in J(t) can be removed, giving

$$J(t) = \int_{-1}^{*1} \frac{\theta(\tau)\, d\tau}{(\tau - t)(\tau t - 1)} = \int_{-1}^{1} \frac{\theta(\tau) - \theta(t)}{(\tau - t)(\tau t - 1)} d\tau .$$

$$= \int_{-1}^{T} \frac{\theta(\tau) - \theta(t)}{(\tau - t)(\tau t - 1)} d\tau + \int_{T}^{1} \frac{\theta(\tau) - \theta(t)}{(\tau - t)(\tau t - 1)} d\tau . \tag{16}$$

If we let the chord of AP be ℓ_1 and the chord of PB be ℓ_2†, then

$$\ell_1 = 2A \int_{-1}^{T} \left| \frac{1 - Tt}{T - t} \right|^{\epsilon} g(t; t_o) \left\{ \exp\left[\frac{(1 - t^2)}{\pi} J_1(t) \right] \cos \theta_1(t) \right\} dt$$

and (17)

$$\ell_2 = 2A \int_{T}^{1} \left| \frac{1 - Tt}{T - t} \right|^{\epsilon} g(t; t_o) \left\{ \exp\left[\frac{(1 - t^2)}{\pi} J_2(t) \right] \cos \theta_2(t) \right\} dt$$

where ℓ_1, ℓ_2, θ_1 and θ_2 are shown in Fig. 1c. For given U, α, $\theta(x)$, ℓ_1 and ℓ_2, Eqs. (2), (3) and (17) provide a set of functional equations

† The subscripts 1 and 2 in all following equations refer to the main foil and the flap respectively.

for unknown t_o, $c(\tau)$, A and T.

To facilitate the numerical computation of the above integrals it is convenient to introduce the following changes of variables

$$t_1(x) = \frac{T - x^2}{1 - Tx^2}, \quad t_2(x) = \frac{T + x^2}{1 + Tx^2}; \tag{18}$$

so that t_1 varies from T to -1, t_2 from T to +1, as x increases from 0 to 1. Then Eq. (17) may be written as

$$\ell_k = 4A(1 - T^2)I_k \tag{19}$$

where, with k = 1, 2,

$$I_k = \int_o^1 \frac{x^{(1-2\epsilon)}}{[1 + (-)^k Tx^2]^2} \frac{g(t_k(x); t_o)}{V^4} \left\{ \exp\left[\frac{1 - t_k^2}{\pi} J_k(x) \right] \cos \theta_k(x) \right\} dx, \tag{20}$$

$$J_1(x) = 2(1 - T^2) \left\{ \int_o^1 \frac{[\theta_1(u) - \theta_1(x)]\, u\, du}{(\tau_1 - t_1)(\tau t_1 - 1)(1 - Tu^2)^2} + \int_o^1 \frac{[\theta_2(u) - \theta_1(x)]\, u\, du}{(\tau_2 - t_1)(\tau_2 t_1 - 1)(1 + Tu^2)^2} \right\},$$

and (21)

$$J_2(x) = 2(1 - T^2) \left\{ \int_o^1 \frac{[\theta_1(u) - \theta_2(x)]\, u\, du}{(\tau_1 - t_2)(\tau_1 t_2 - 1)(1 - Tu^2)^2} + \int_o^1 \frac{[\theta_2(u) - \theta_2(x)]\, u\, du}{(\tau_2 - t_2)(\tau_2 t_2 - 1)(1 + Tu^2)^2} \right\}.$$

$\theta_1(x)$ and $\theta_2(x)$ in Eqs. (20) and (21) are the angles between the tangents and the chords of AP and PB at $c_1(x)$ and $c_2(x)$ respectively, as shown in Fig. 1(c).

If we now normalize the total chord $(\ell_1 + \ell_2)$ to be unity, we have

$$A = \frac{1}{4(1 - T^2)(I_1 + I_2)}; \tag{22}$$

and hence

$$c_k(y) = \frac{1}{I_1+I_2}\int_o^y \frac{x^{(1-2\epsilon)}}{[1+(-)^k Tx^2]^2}\ \frac{g(t_k(x);t_o)}{V^4}\left\{\exp\left[\frac{1-t_k^2}{\pi}J_k(x)\right]\cos\theta_k(x)\right\}dx,$$

$(k = 1,2)$ (23)

The ratio of the flap chord f to the total chord c is

$$f/c = \frac{I_2}{I_1+I_2} = \frac{I_2}{I_1+I_2}\ . \tag{24}$$

Making the same changes of variable, Eqs. (9) and (11) become

$$V_a = \exp\left\{\frac{2}{\pi}(1-T^2)\left[\int_o^1 Q(t_1(x))\ \frac{x\theta_1(x)\,dx}{(1-Tx^2)^2} + \int_o^1 Q(t_2(x))\frac{x\theta_2(x)\,dx}{(1+Tx^2)^2}\right]\right\} \tag{25}$$

and

$$\beta_a = -\frac{2}{\pi}V\sin\beta(1-T^2)\left[\int_o^1 H(t_1(x))\frac{x\theta_1(x)\,dx}{(1-Tx^2)^2} + \int_o^1 H(t_2(x))\frac{x\theta_2(x)\,dx}{(1+Tx^2)^2}\right], \tag{26}$$

where Q and H are given by Eqs. (14) and (15) respectively.

The pressure coefficient at any point is

$$C_p = \frac{p-p_c}{\frac{1}{2}\rho U^2} \tag{27}$$

where p is the pressure at the wetted surface of the plate and p_c the constant pressure in the cavity. From the Bernoulli equation we obtain

$$C_p = U^{-2}\ (1-q^2) = (1+\sigma)(1-q^2) \tag{28a}$$

or

$$C_p = (1+\sigma)(1 - w\overline{w}) , \tag{28b}$$

where σ is the wake under-pressure coefficient, or the cavitation number for cavity flows, given by $\sigma = \frac{p_\infty - p_c}{\frac{1}{2}\rho U^2}$, and $\overline{w}$ is the complex conjugate of w.

The complex force coefficient for the main body, $C_{x_1} + iC_{y_1}$, can be written as

$$C_{x_1} + iC_{y_1} = i\int_A^P C_p\, dz = i(1+\sigma)\int_A^P (1 - w\overline{w})\, dz$$

$$= i(1+\sigma)\left[(z_P - z_A) - \int_{-1}^{T} \overline{w}\ \frac{df}{dt}\, dt\right] , \tag{29}$$

From Eqs. (1), (4), (22) and the transformation (18), we can write the above equation as

$$C_{x_1} + iC_{y_1} = i(1+\sigma)\left[\ell_1 - \frac{1}{I_1 + I_2}\int_0^1 x^{(1+2\epsilon)}\, t_1^{\,2}(x)\ \frac{g(t_1(x); t_o)}{V^4}\ \exp\left\{-\frac{[1 - t_1^{\,2}(x)]}{\pi} J_1(x)\right\} e^{i\theta_1}\, dx\right] . \tag{30a}$$

Similarly, the complex force coefficient for the flap, $C_{x_2} + iC_{y_2}$, becomes

$$C_{x_2} + iC_{y_2} = i(1+\sigma)e^{-i\epsilon\pi}\left[\ell_2 - \frac{1}{I_1 + I_2}\int_0^1 x^{(1+2\epsilon)}\, t_2^{\,2}(x)\ \frac{g(t_2(x); t_o)}{V^4}\ \exp\left\{-\frac{[1 - t_2^{\,2}(x)]}{\pi} J_2(x)\right\} e^{i\theta_2}\, dx\right] . \tag{30b}$$

The lift and drag coefficients, C_L and C_D, are given by

$$C_D + iC_L = [(C_{x_1} + iC_{y_1}) + (C_{x_2} + iC_{y_2})]\, e^{-i\alpha} . \tag{31}$$

Special Case: Flat Plate

As a special case, we now consider a flat plate with a flap as shown in Fig. 2. This configuration is particularly simple since $\theta = 0$ everywhere along the chord. By putting $\theta = 0$ in our formulae, V_a given by Eq. (9) becomes unity and β_a given by Eq. (11) becomes zero so that

$$V = V_f \tag{32}$$

and

$$\beta = \beta_f , \tag{33}$$

where V_f and β_f are given by Eqs. (8) and (10) respectively. Similarly w, I_1, I_2, c_1 and c_2 are given by Eqs. (1b), (20) and (23) with the factor inside the curly brackets equal to unity.

From the above and Eq. (28b) we obtain the pressure coefficient

$$C_p = (1+\sigma)\left[1 - t^2 \left|\frac{T-t}{1-Tt}\right|^{2\epsilon}\right] . \tag{34}$$

In terms of the variable x defined by Eq. (18), Eq. (34) may be written as

$$C_{p_k}(x) = (1+\sigma)\left[1 - t_k^{\,2}(x)\, x^{4\epsilon}\right] , \qquad (k = 1,2). \tag{35}$$

The moment coefficients about the hinge point P due to the pressure over the main foil, AP, and of the flap, PB, as shown in Fig. 2, are

$$C_{M_i} = \int_{-1}^{T} C_{p_i}(t)\, c_i(t)\, dc_i$$

and

$$C_{M_2} = \int_T^{1} C_{p_2}(t)\, c_2(t)\, dc_2$$

respectively. From Eq. (23) we get

$$C_{M_k} = \frac{1}{(I_1 + I_2)^2} \int_o^1 C_{p_k}(x) \frac{x^{(1-2\epsilon)}}{[1 + (-)^k T x^2]^2} \frac{g(t_k(x); t_o)}{V^4} \int_o^x \frac{y^{(1-2\epsilon)}}{[1 + (-)^k T y^2]^2} \frac{g(t_k(y); t_o)}{V^4}\, dy\, dx,$$

$(k = 1, 2)$ (37)

where I_1 and I_2 are given by Eq. (20) with the factor inside the curly brackets equal to unity and $g(t; t_o)$ is given by Eq. (4).

It is also desirable to know the location of the centers of pressure of both the main body and the flap as well as the total forces at those points. Let a_1 and a_2 be the distances from the hinge point, P, to the center of pressure on the main foil and to that on the flap respectively, and let C_{F_1} and C_{F_2} be the force coefficients acting at these points. We may now write

$$C_{F_1} = \int_{-1}^{T} C_p\, dc, \quad C_{F_2} = \int_T^{1} C_p\, dc,$$

with the help of Eq. (23) the final results are

$$C_{F_k} = \frac{1}{I_1 + I_2} \int_o^1 C_{p_k}(x) \frac{x^{(1-2\epsilon)}}{[1 + (-)^k T x^2]^2} \frac{g(t_k(x); t_o)}{V^4}\, dx, \quad (k = 1, 2),$$

(38)

$$a_k = C_{M_k} / C_{F_k}, \quad (k = 1, 2). \tag{39}$$

Knowing these quantities we can transfer the total moment to the leading edge, giving

$$C_{M_{LE}} = C_{F_1}(\ell_1 - a_1) + C_{F_2}(\ell_1 \cos\epsilon\pi + a_2), \tag{40}$$

where $C_{M_{LE}}$ is considered to be positive in the nose down sense. The hinge moment is defined as the moment of the flap about the hinge point, hence

$$C_{M_H} = C_{M_2}. \tag{41}$$

The pressure distribution is given in the parametric form $s(x)$, $C'_p(x)$, where $s(x)$ denotes the length along the foil surface measured from the leading edge such that $0 \leq s \leq 1$,

$$\begin{aligned} s(x) &= 1 - \frac{f}{c} - c_1(x) \quad \text{on AP} \\ &= 1 - \frac{f}{c} + c_2(x) \quad \text{on PB} \end{aligned} \tag{42}$$

and C'_p is the pressure coefficient which is defined as unity at the stagnation point D and is equal to negative σ on the cavity side. Then we have

$$C'_{p_k}(x) = (1+\sigma)\left[1 - t_k^2(x)x^{4\epsilon}\right] - \sigma, \quad (k = 1,2). \tag{43}$$

The lift and drag coefficients are given by (refering to Eq. (78) of Ref. (8))

$$C_L = \frac{\pi A}{U^2}\,\frac{(U^{-1} + U)\csc\beta}{(V^{-2} + V^2 - 2\cos 2\beta)}\left\{\cos\beta + \frac{\epsilon(1-T^2)[(1+T^2)V^2\cos\beta - TV(1+V^2)\cos 2\beta]}{(T^2+V^2-2tV\cos\beta)(T^2V^2+1-2tV\cos\beta)}\right\} \tag{44}$$

$$C_D = \frac{\pi A}{U^2} \frac{(U^{-1} - U)/(1 - V^2)}{(V^{-2} + V^2 - 2\cos 2\beta)} \left\{ 1 + V^2 + \frac{\epsilon(1 - T^2)[(1 + T^2)V^2(1 + V^2) - 2TV\cos\beta(1 + V^4)]}{(T^2 + V^2 - 2TV\cos\beta)(T^2V^2 + 1 - 2TV\cos\beta)} \right\} \tag{45}$$

where A is given by Eq. (22).

Numerical Procedures:

a) Flat plate with a flap.

A double iteration procedure is required to evaluate the force coefficients for prescribed U, α, ϵ and f/c. We first solve the inverse problem: choose U, α, ϵ and T as the independent parameters, solve for V and β (hence t_o) by iterating the parametric relations in Eqs.(32) and (33). We then obtain the corresponding flap-to-chord ratio, f/c $= I_2/(I_1 + I_2)$, where I_1 and I_2 are given by Eq. (20) with the factors inside the curly brackets equal to unity. A type of iteration similar to Newton's method is then used on T to find V and β corresponding to the desired value of f/c.

Once V and β are established, the moment coefficients, $C_{M_{LE}}$ and C_{M_H}, are obtained f qs. (37)-(41), the pressure distribution from Eqs. (42) and (43) ar ft and drag coefficients from Eqs. (44) and (45).

The details of the cal ions outlined above are described in Appendix A*.

* The program listing is available upon request.

b) Arbitrary profile.

The iteration scheme for the arbitrary profile is a combination of the above method and the approximate scheme of Wu and Wang [9] and is described in detail in Appendix B*.

Results:

The numerical calculations outlined above were carried out for three models of flapped flat plate hydrofoils with flap to chord ratios of 0.2, 0.4 and 0.6. For each model the flap angle, $\epsilon\pi$, was varied from 10° to 60° and the angle of attack, α, from 5° to 60° for cavitation numbers between 0 and 1.0**.

Figures 3 through 5 show the total moment coefficient about the leading edge, $C_{M_{LE}}$, and the moment of the flap about the hingepoint, C_{M_H}, as functions of σ for $\alpha = 5^\circ$ through 60°. For each model the flap angles 10°, 20°, 40° and 60° are shown. $C_{M_{LE}}$ as a function of $\epsilon\pi$. is given in Fig. 6 for all three models at various cavitation numbers for $\alpha = 10^\circ$, 20° and 30°. Figure 7 shows the lift coefficient. C_L, versus $\epsilon\pi$ for the same conditions. The polar plots of C_L/C_D versus C_L for $\sigma = 0$ are shown in Fig. 8, in which the solid lines are lines of constant α and the dashed lines are those of constant $\epsilon\pi$. Since, within the range of the cavitation numbers concerned, C_L/C_D is almost independent of σ, no corresponding curves are needed for other values of σ.

Some typical pressure distribution curves for the model with

---

* The program listing is available upon request.

** Tabulated results are available upon request.

f/c = 0.2 at $\alpha = 10^{\circ}$ and $\epsilon_T = 0^{\circ}$, 20°, 40° and 60° are shown in Fig. 9. The experimental points are taken from the work by Meijer [10]. In Meijer's experiments, different sized models were tested in order to make wall effect corrections. In Fig. 9 the theoretical results agree very well with the experimental ones, except around the hinge region. The discrepancy there may be attributed to viscous effect. Curves were faired through Meijer's experimental points, given in Fig. 9, and then integrated to obtain C_L and C_D. The results are plotted along with the corresponding theoretical lift and drag curves in Fig. 10. As would be expected from the pressure distribution correlation in Fig. 9, the agreement in C_L and C_D is very good.

Figure 11 illustrates the agreement between Parkin's experiment [11] and the theory of $C_{M_{LE}}$ as a function of σ for a flat plate at angles of attack from 10° to 30°. The experimental points of Parkin's experiment have not been corrected for wall effects.

Besides the above comparisons between two-dimensional results, it is also interesting to compare the present two-dimensional theoretical results with experiments having three-dimensional effect. Wetzel and Maxwell [7] performed experiments with ventilated finite aspect ratio models at different submergences in a free jet. Some of these results are shown in Figs. 12 and 13. In general, the agreement between the two-dimensional theory and three-dimensional flow is not as good as the agreement with the two-dimensional experiments of Parkin and Meijer, but as aspect ratio and submergence are increased the agreement tends to improve.

ACKNOWLEDGMENT

The authors wish to express their sincere thanks to Professor T. Y. Wu for his many helpful suggestions and his guidance in this problem, to Miss Cecilia Lin for the drawings and to Mrs. Mary Goodwin for typing the manuscript.

REFERENCES

1. Tulin, M. P. & Burkart, M. P., "Linearized theory for flows about lifting foils at zero cavitation number," Department of the Navy, David W. Taylor Model Basin, Report C-638, 1955.

2. Johnson, Jr., V. E., "Theoretical and experimental investigation of arbitrary aspect ratio, supercavitating hydrofoils operating near the free water surface," NACA RM L57116, 1957.

3. Auslaender, J., "The behavior of supercavitating foils with flaps operating at high speed near a free surface." Hydronautics, Inc. Rockville, Md. TR 001-2, 1960.

4. Lin, J. D., "A free streamline theory of flows about a flat plate with a flap at zero cavitation number." Hydronautics, Inc., Rockville, Md. TR 119-3, 1961.

5. Brown, P. W., "A model investigation of the force characteristics of a hydrofoil with various flap configurations." Stevens Institute of Technology, Davidson Laboratory Report LR-757, 1959.

6. Conolly, A. C., "Experimental investigations of supercavitating hydrofoils with flaps." General Dynamics/Convair, San Diego, Report GDC-63-210, 1963.

7. Wetzel, J. M. & Maxwell, W. H. C., "Force characteristics of flapped, ventilated hydrofoils in smooth and rough water." St. Anthony Falls Hydraulic Laboratory, University of Minnesota, Report 66, 1963.

8. Wu, T. Y. & Wang, D. P., "A wake model for free-streamline flow theory, Part 2. Cavity flows past obstacles of arbitrary profile." J. Fluid Mechanics, Vol. 18, 65-93, 1964.

9. Wu, T. Y. & Wang, D. P., "A approximate numerical scheme for the theory of cavity flows past obstacles of arbitrary profile." Trans. ASME, J. Basic Eng. Vol. 86, Ser D, No. 3, 556-560, 1964.

10. Meijer, M. C., "Pressure measurement on flapped hydrofoils in cavity flows and wake flows." California Institute of Technology Report E-133.2, 1965.

11. Parkin, B. R., "Experiments on circular-arc and flat-plate hydrofoils in non-cavitating and full cavity flows." California Institute of Technology, Report 47-7, 1956. (see also J. Ship Res. 1, 34-56, 1958.)

APPENDIX A

The double iteration procedure outlined in the text for the flat plate problem presents no problem when done on a high speed computer. All calculations presented here were done on the IBM 7094 at Booth Computing Center, California Institute of Technology.

Choose U, α, ϵ and let the first approximation of T be 0.5, then calculate V and β by iteration of Eqs. (32) and (33). Since V and β are rather close to U and α in value, let $V^{(0)} = U$ and $\beta^{(0)} = \alpha$ be the first approximations, then

$$V^{(1)} = V_f(T, V^{(0)}, \beta^{(0)})$$

and

$$\beta^{(1)} = \beta_f(T, V^{(0)}, \beta^{(0)})$$

are the next approximations. Continue this procedure until $| V^{(n-1)} - V^{(n)} |$ and $| \beta^{(n-1)} - \beta^{(n)} |$ are less than the allowable error. This iteration converges very well; on the average about 6 iterations will produce an accuracy such that the error is less than 0.00001.

Once V and β are determined the corresponding flap to chord ratio, f/c, can be calculated from Eq. (24), where I_1, and I_2 are given by Eq. (20) with the curly brackets equal to one. Let the desired f/c be R and the first approximations to T and f/c be $T^{(0)}$ and $R^{(0)}$ respectively. Since f/c decreases as T increases, the second approximation to T is arbitrarily set to be either

$$T^{(1)} = 0.1; \quad R - R^{(0)} > 0$$

or

$$T^{(1)} = 0.9; \quad R - R^{(0)} < 0.$$

The corresponding $R^{(1)}$ is calculated from the first iteration process and now we can apply a modified Newton's method,

$$T^{(2)} = T^{(0)} + [R - R^{(0)}] \left[\frac{T^{(0)} - T^{(1)}}{R^{(0)} - R^{(1)}} \right]$$

and

$$R^{(2)} = \frac{f}{c} \quad (T^{(2)}).$$

Continue these successive approximations of T according to

$$T^{(n+1)} = T^{(n-1)} + [R - R^{(n-1)}] \left[\frac{T^{(n-1)} - T^{(n)}}{R^{(n-1)} - R^{(n)}} \right]$$

until $|R - R^{(n-1)}|$ is less than the allowable error.

It should be pointed out here that only positive values of T are of interest for the physical application considered here. If T becomes negative then the stagnation point D has moved to the flap side of the hinge point. This situation occurs when $f/c \to 1$ and α and ϵ become large.

Once T, V, and β are determined the pressure distribution, lift, drag and moment coefficients are readily calculated as outlined in the text. The numerical integration required was programed using Simpson's rule on increments of $x = 0.005$ and $y = 0.0001$. This increment size was sufficiently small to produce an accuracy of at least ± 0.0001 for all cases that were calculated. A good check of the accuracy is to print out $s_1(x = 1)$ and $s_2(x = 1)$ as these values should be 0 and 1.0 respectively.

APPENDIX B

The iteration procedure required for the arbitrary profile is somewhat longer and more complex than the flat plate problem because of the added slope function, θ. This additional parameter gives rise to an integration in the V and β calculations; furthermore, the chord calculation becomes a double integral. We have used a modification of the approximate numerical scheme originated by Wu and Wang [10]. This modification is necessary because of the additional requirement of fixed f/c so that T cannot be prescribed as it was in that reference.

We first solve the flat plate problem for the prescribed α, σ, ϵ and f/c. This solution gives us a good first approximation for the unknown parameters V, β and T. Using these initial values we now iterate Eqs. (6), (7) and (24) except that the value of c(x), required to determine $\theta(x)$, is the flat plate value given by Eq. (23) with the curly brackets equal to one (since θ is equal to zero). The values so calculated are designated with *. As before we let the prescribed f/c be R and the calculated f/c be $R^{(n)}$. This time we do not iterate V^* and β^* for each value of T^* (and hence R^*) because they are less sensitive than R^* to changes in T^*. It is also necessary to adjust the chord values $c_1(x)$ and $c_2(x)$ at each iteration so that $c_1(x = 1) = 1 - R$ and $c_2(x = 1) = R$. This adjustment in the chord values is necessary because the θ values are defined only in the regions $0 \leq c_1 \leq (1 - R)$ and $0 \leq c_2 \leq R$. With these exceptions this iteration is carried out in the same way as in the flat plate iteration until

$$| V^{*(n-1)} - V^{*(n)} |, \quad | \beta^{*(n-1)} - \beta^{*(n)} | \text{ and } | R^{*(n)} - R |$$

are less than the allowable error. We then calculate the exact value of c(x) (with the curly brackets) and recalculate $V^{(n)}$, $\beta^{(n)}$ and $R^{(n)}$. If necessary this last step is iterated until

$$| V^{(n-1)} - V^{(n)} | \quad | \beta^{(n-1)} - \beta^{(n)} | \text{ and } | R^{(n)} - R |$$

are less than the allowable error. When the camber is small it is found that it is not necessary to iterate this last step.

Our program is written so that the θ values may be obtained either by a four point interpolation from a stored set of θ versus c values or from an analytic expression.

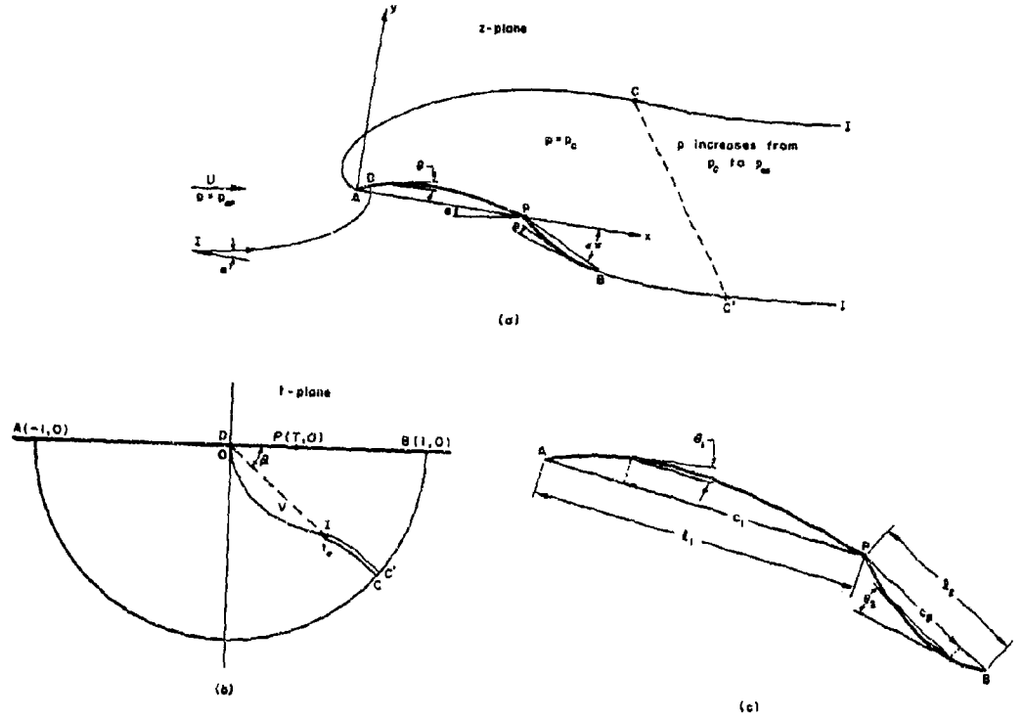

Fig. 1 (a) The free-streamline model for the wake flow past an arbitrary profile with a flap; (b) its mapping in the t-plane and (c) a description of the notations for the foil profile.

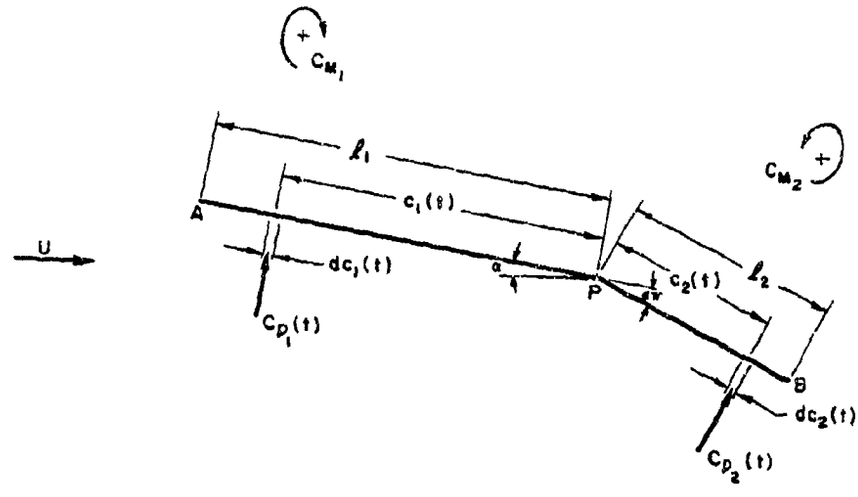

Fig. 2 The coordinate system and notations for a flat plate with a flap.

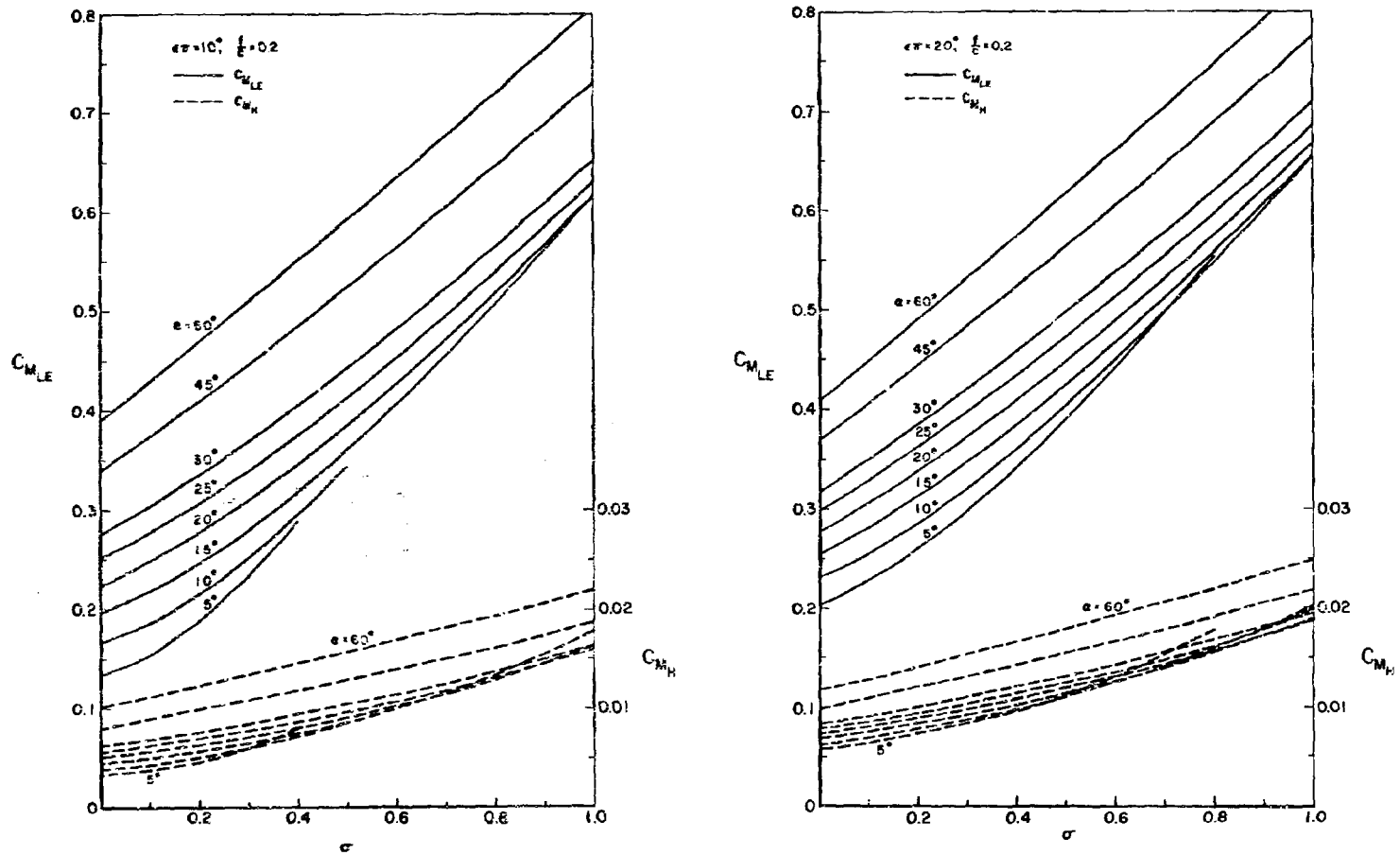

Fig. 3 The variation of $C_{M_{LE}}$ and C_{M_H} with σ, α and ϵ_T for a flapped flat plate with f/c = 0.2.

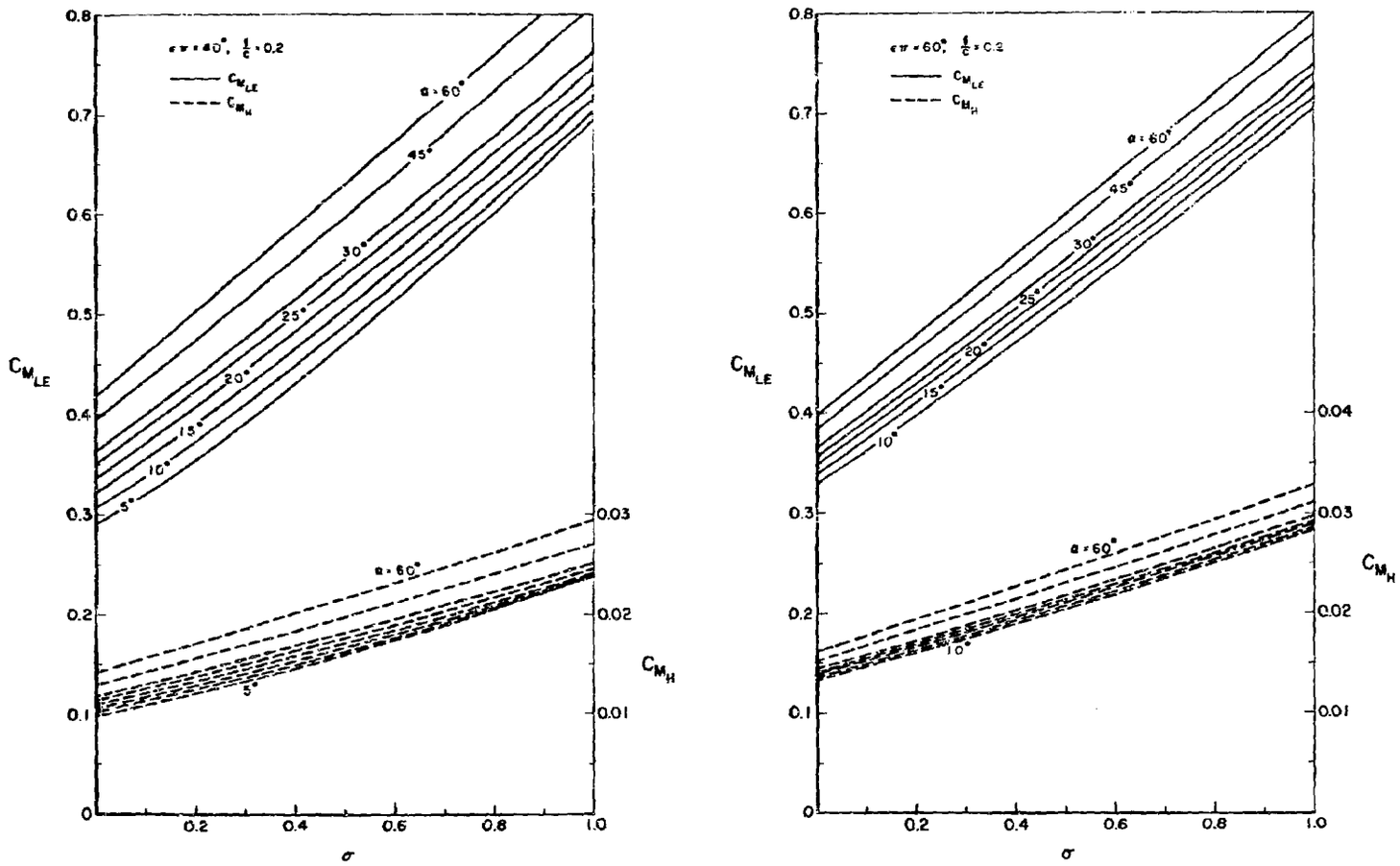

Fig. 3 Continued

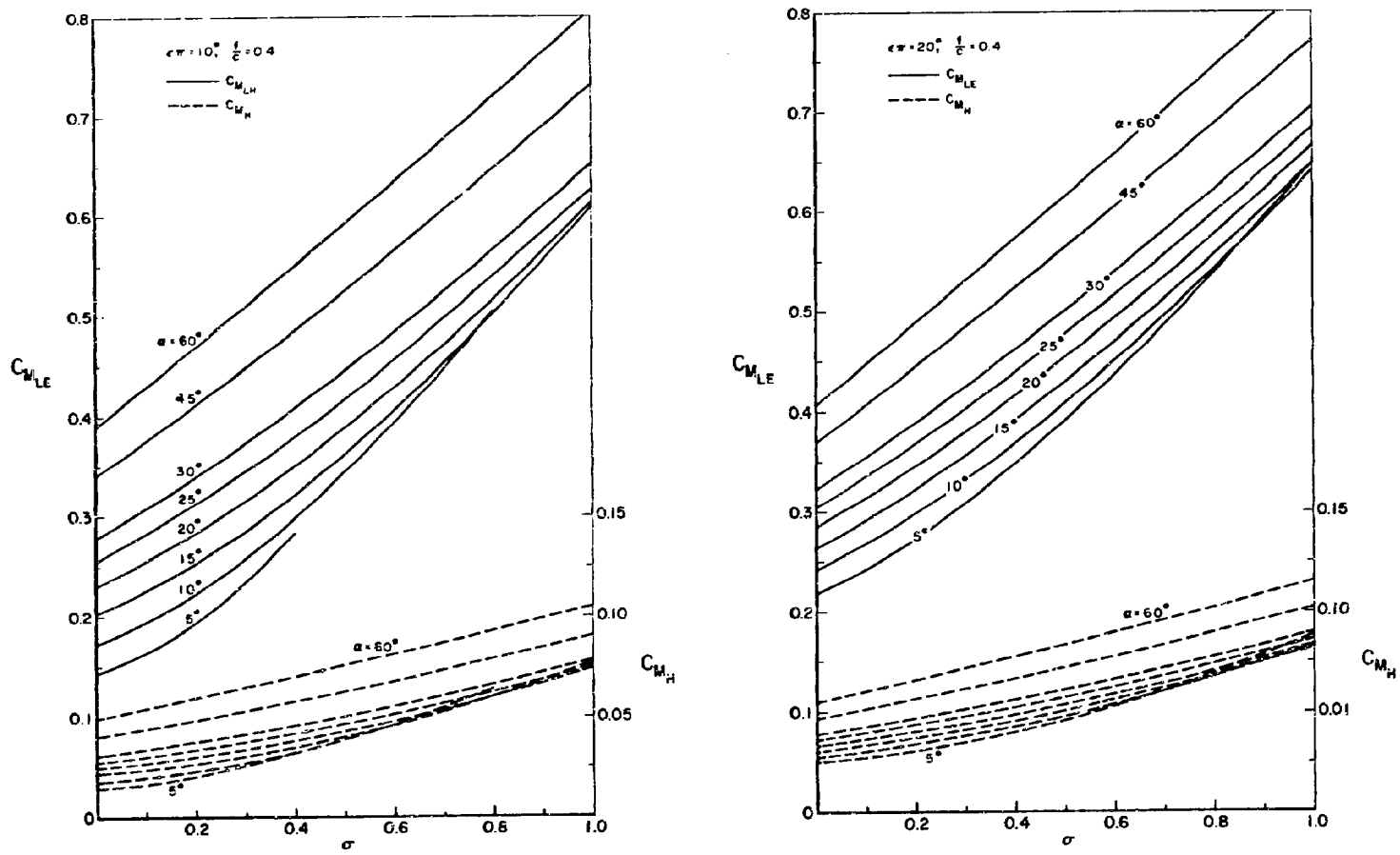

Fig. 4 The variation of $C_{M_{LE}}$ and C_{M_H} with σ, α and ϵ_T for a flapped flat plate with f/c = 0.4.

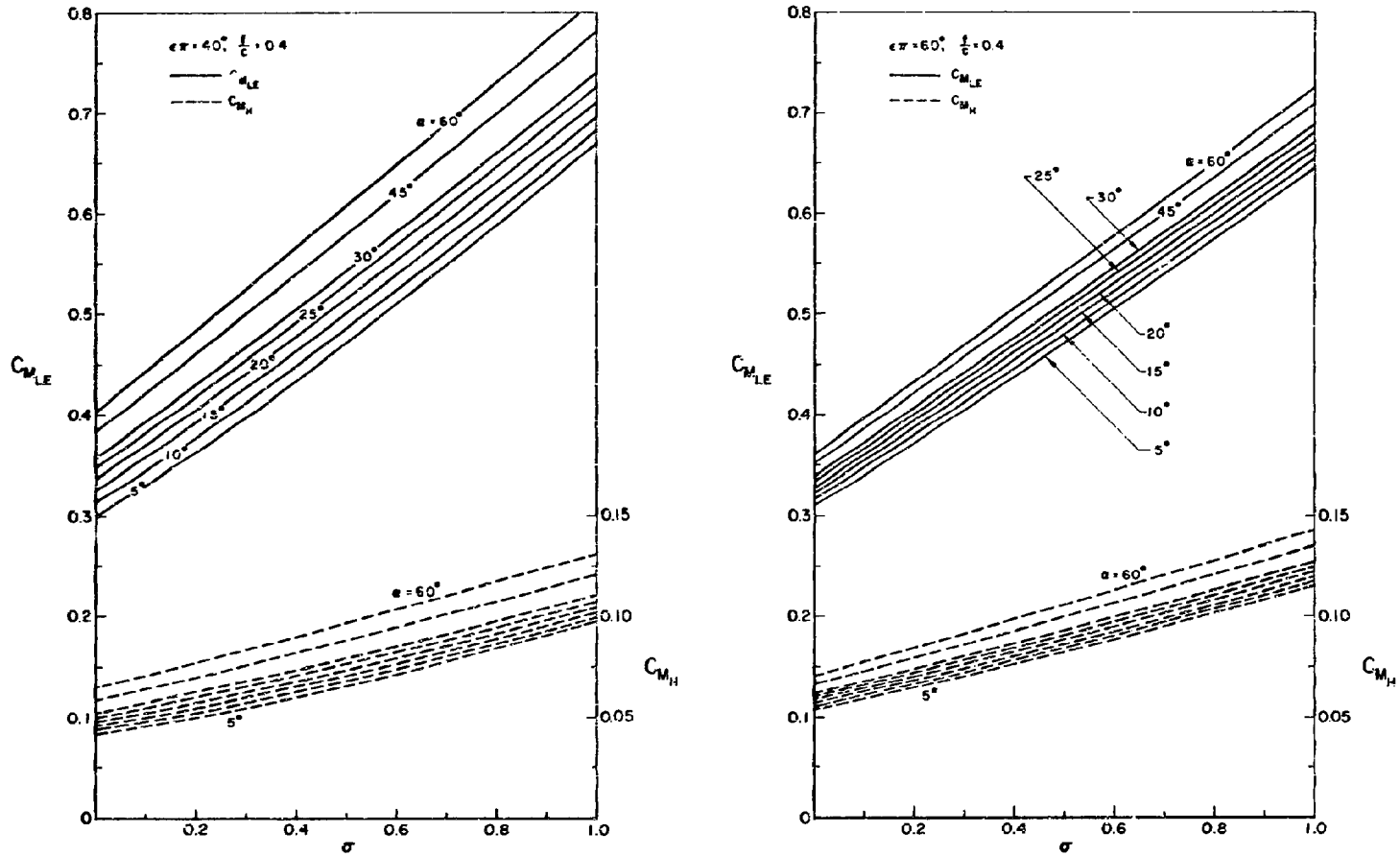

Fig. 4 Continued

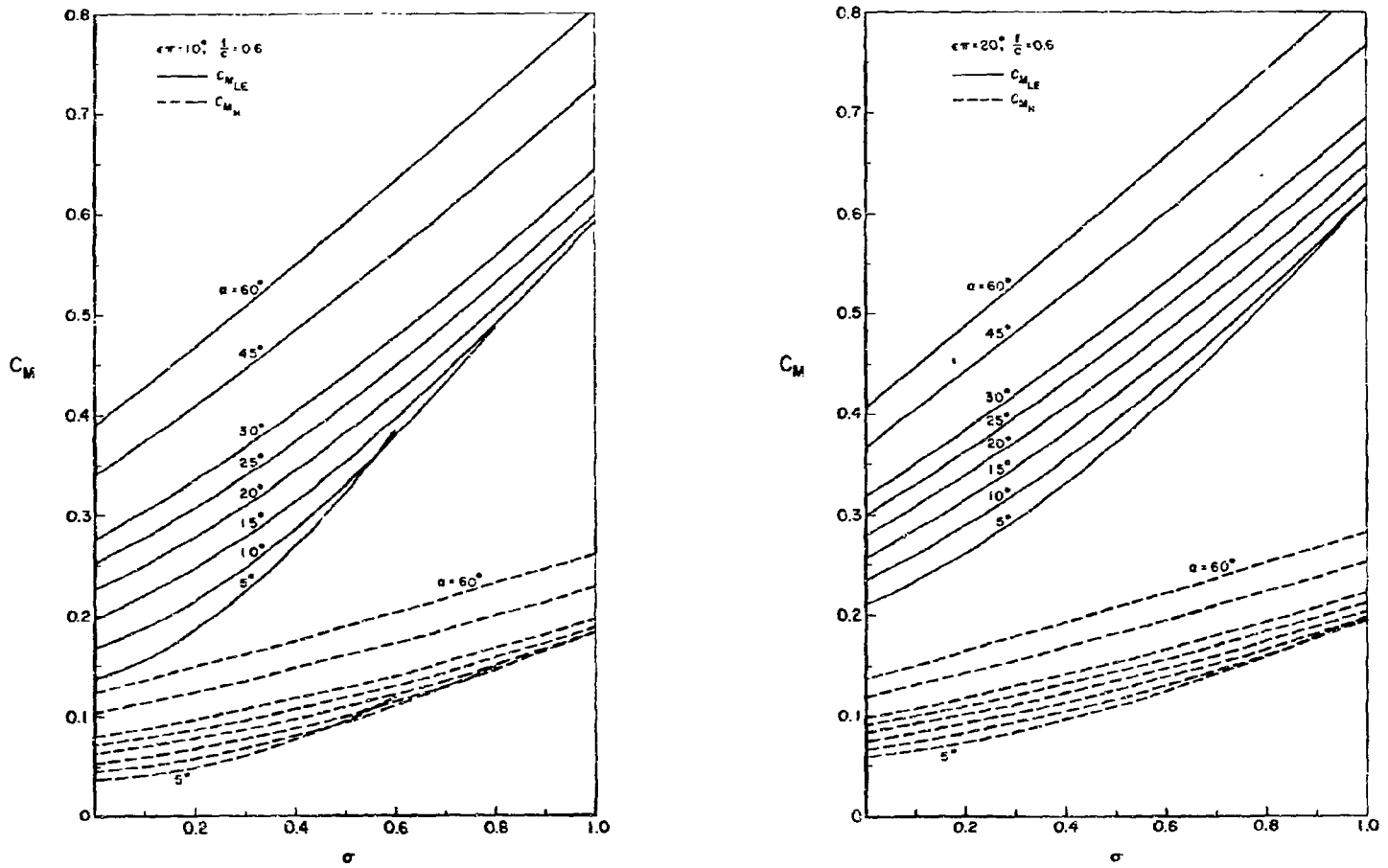

Fig. 5 The variation of $C_{M_{LE}}$ and C_{M_H} with σ, α and ϵ_π for a flapped flat plate with f/c = 0.6.

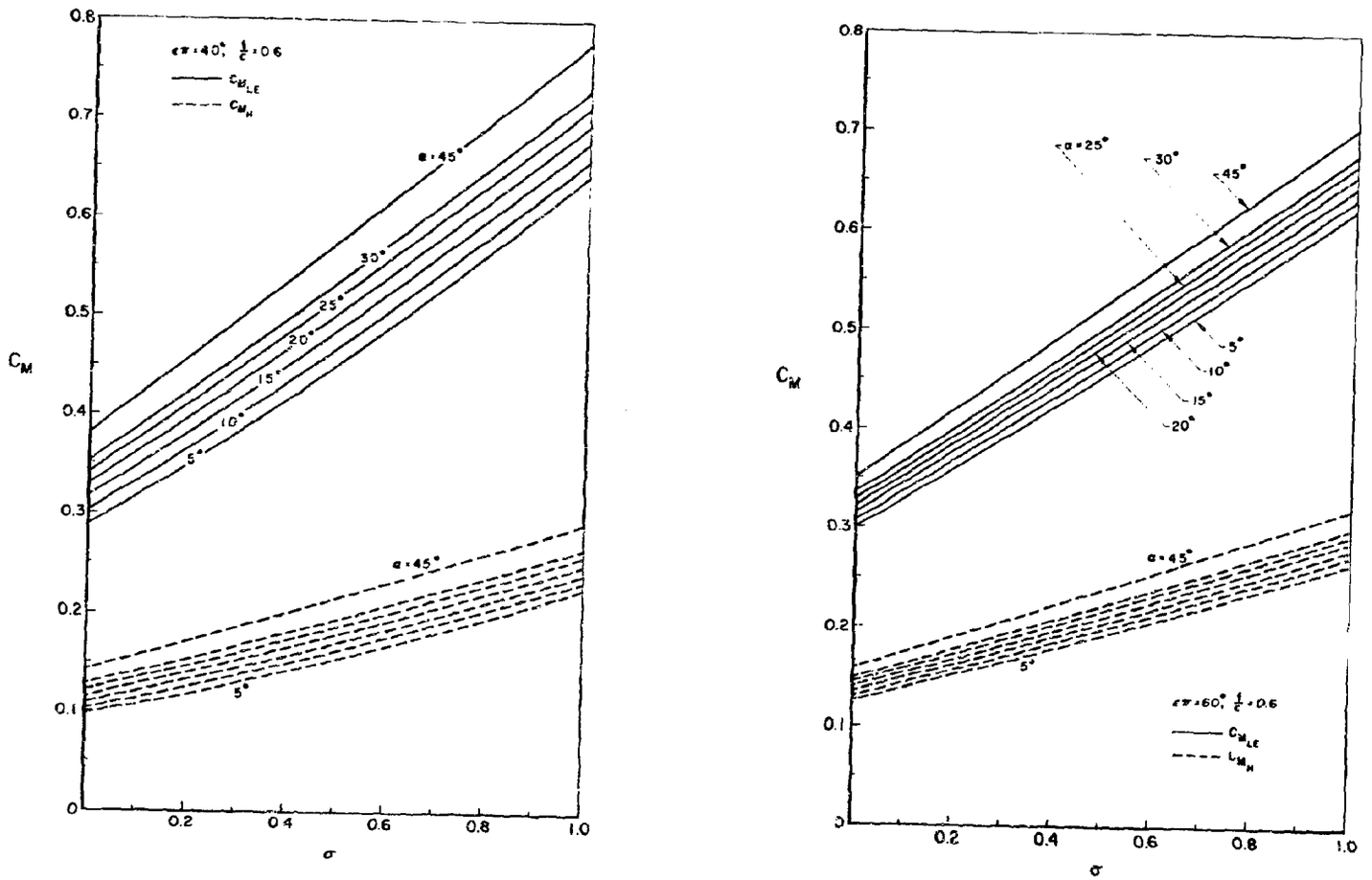

Fig. 5 Continued

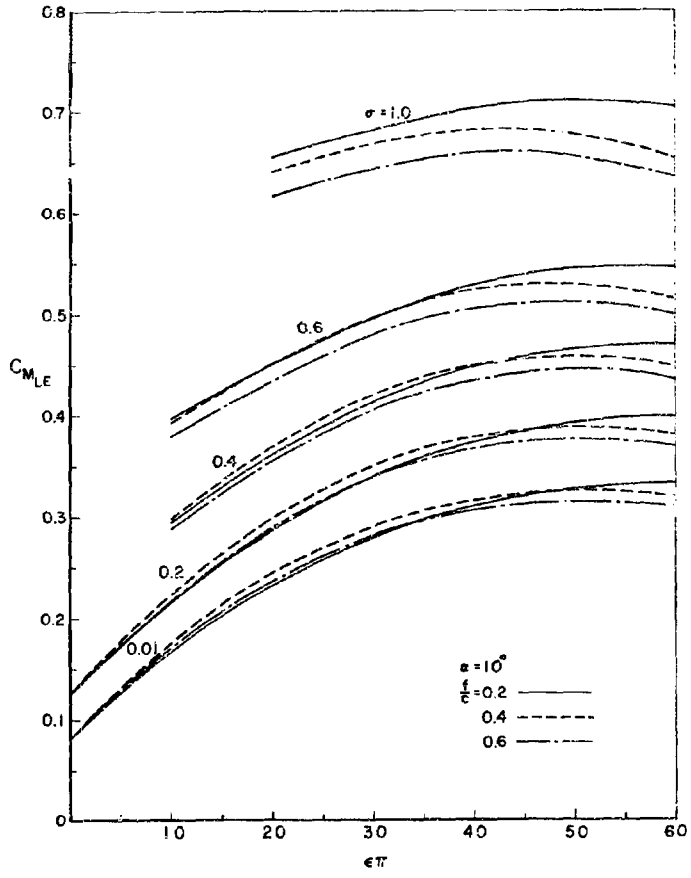

Fig. 6 The variation of $C_{M_{LE}}$ with $\epsilon\pi$ for the flapped flat plate

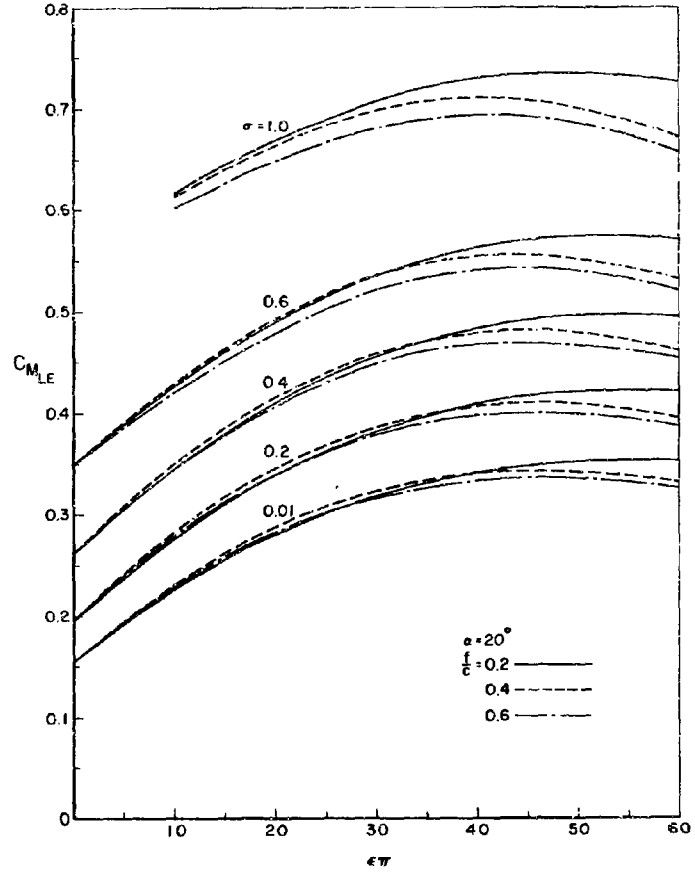

Fig. 6 Continued

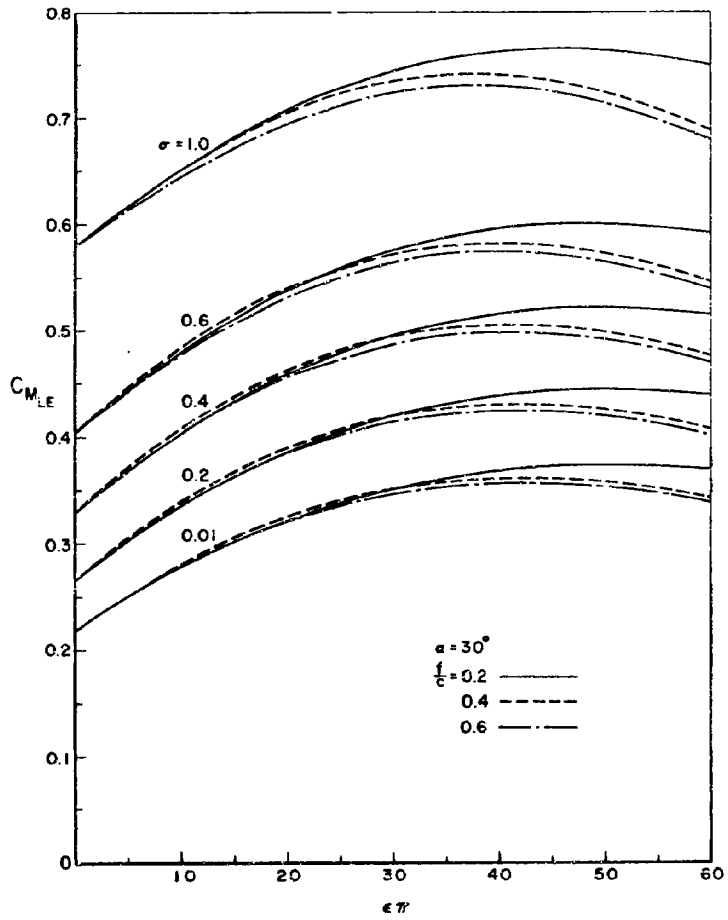

Fig. 6 Continued

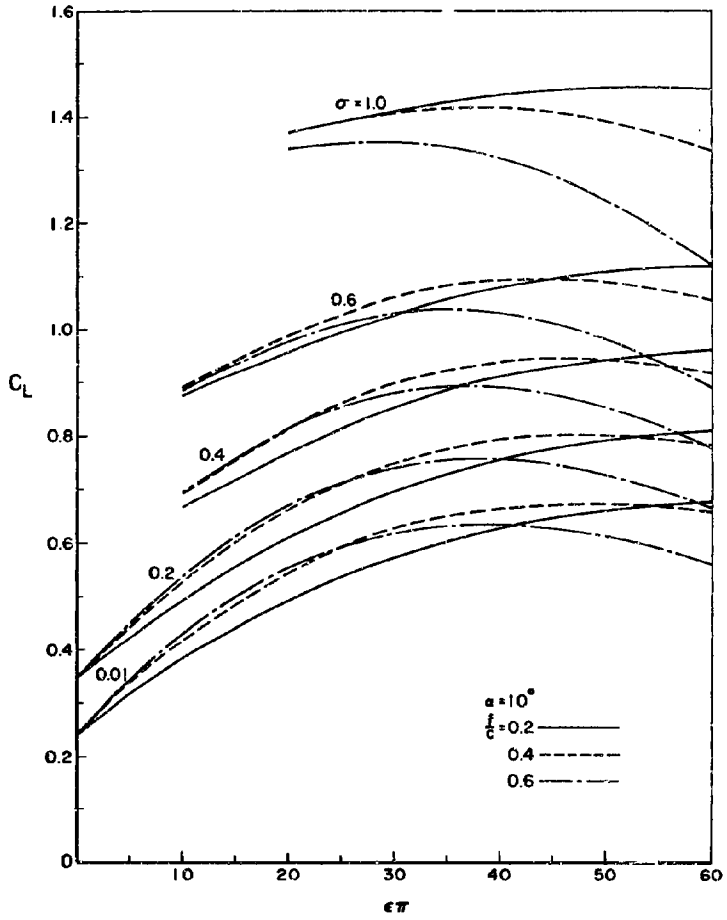

Fig. 7 The variation of C_L with $\epsilon\pi$ for the flapped flat plate.

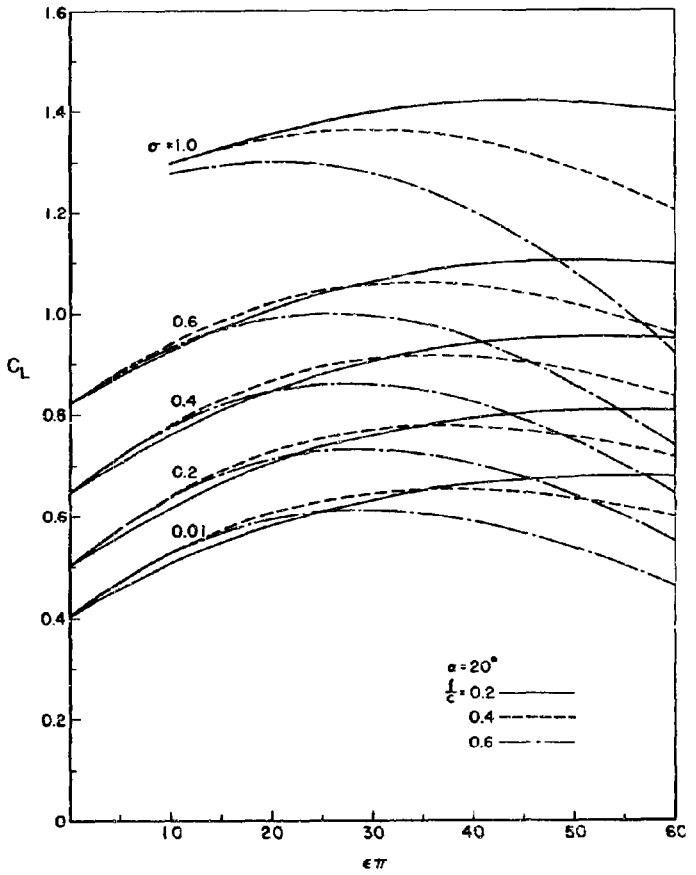

Fig. 7 Continued

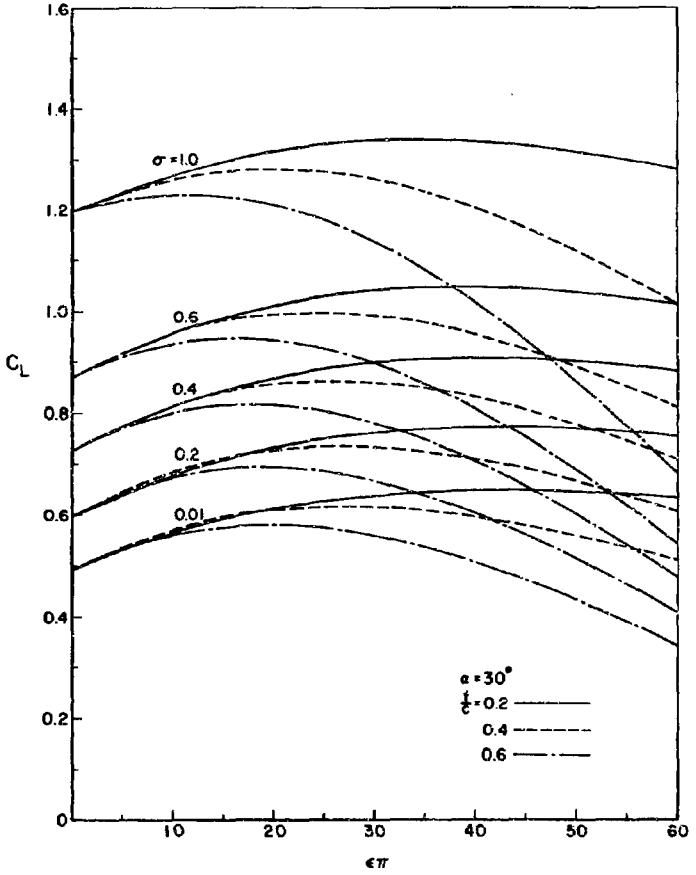

Fig. 7 Continued

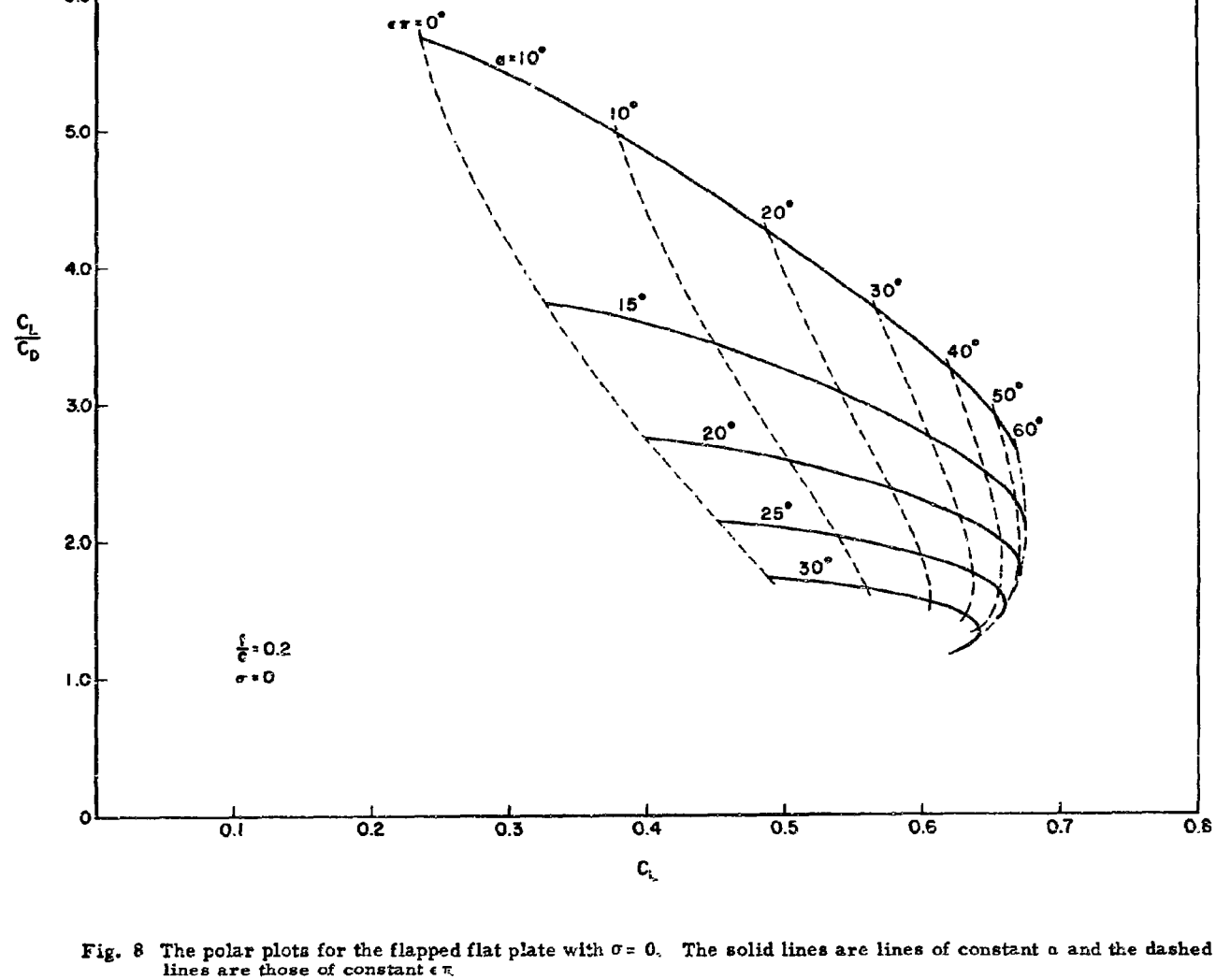

Fig. 8 The polar plots for the flapped flat plate with $\sigma = 0$. The solid lines are lines of constant α and the dashed lines are those of constant $\epsilon\pi$.

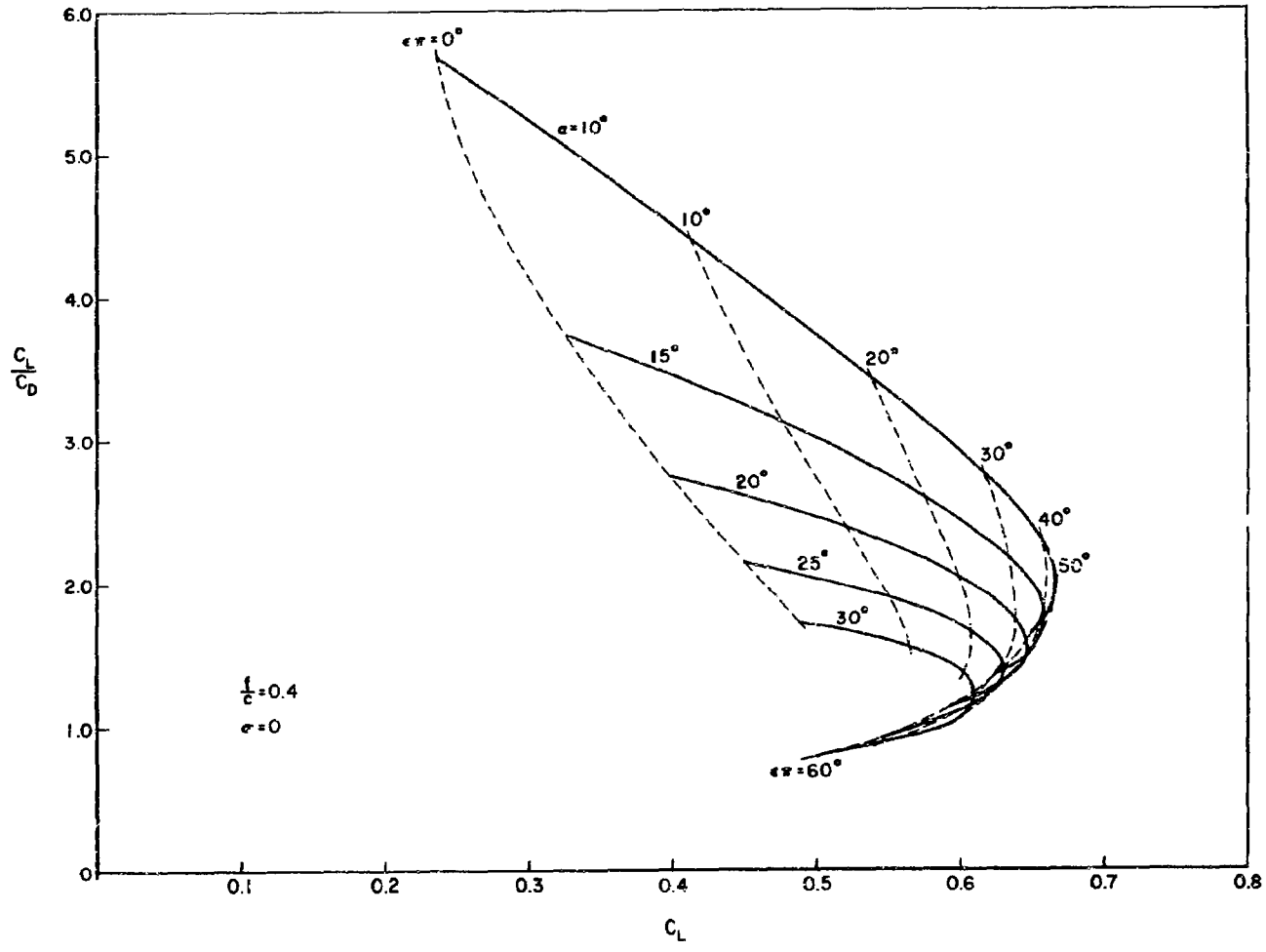

Fig. 8 Continued

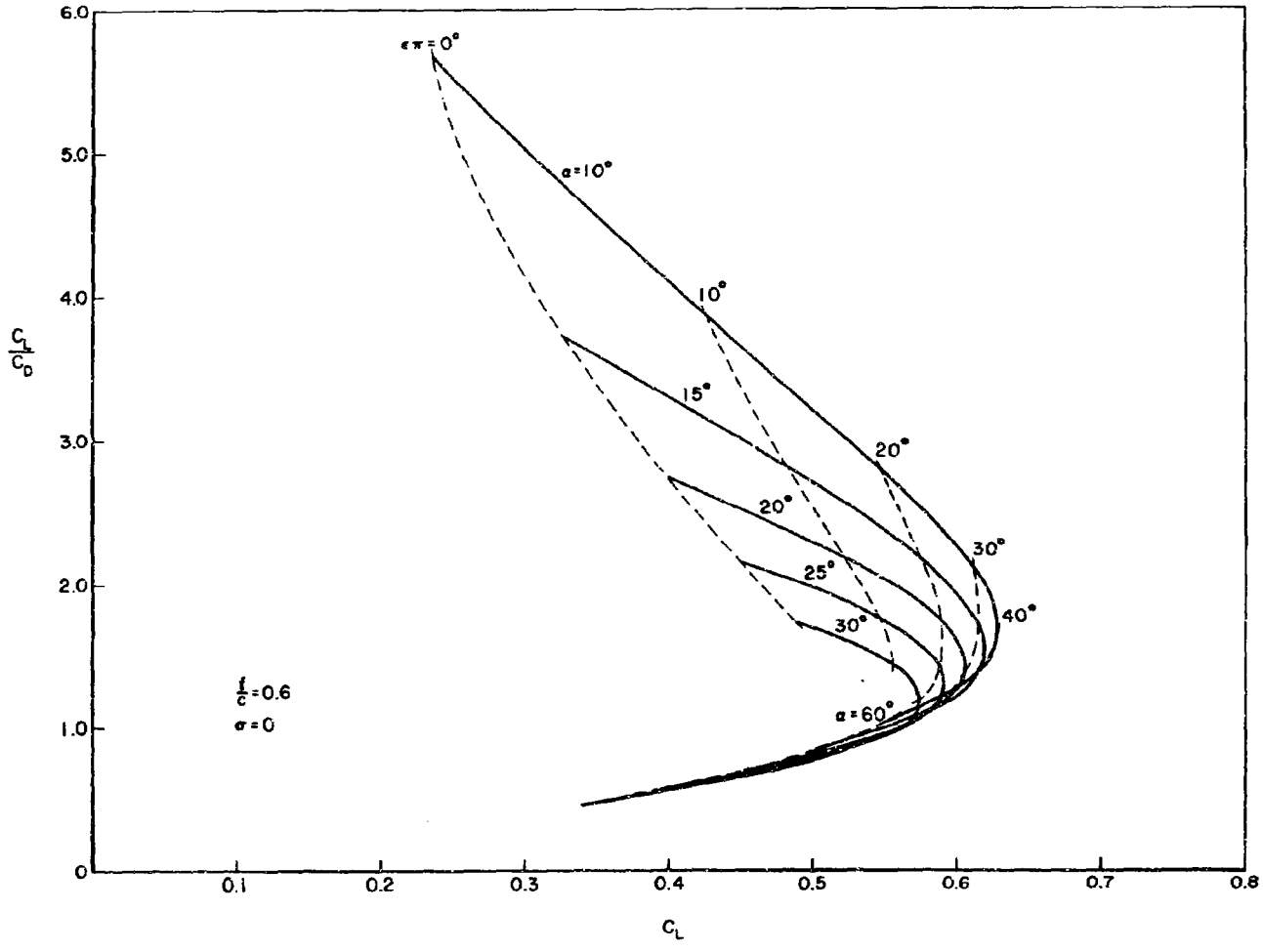

Fig. 8 Continued

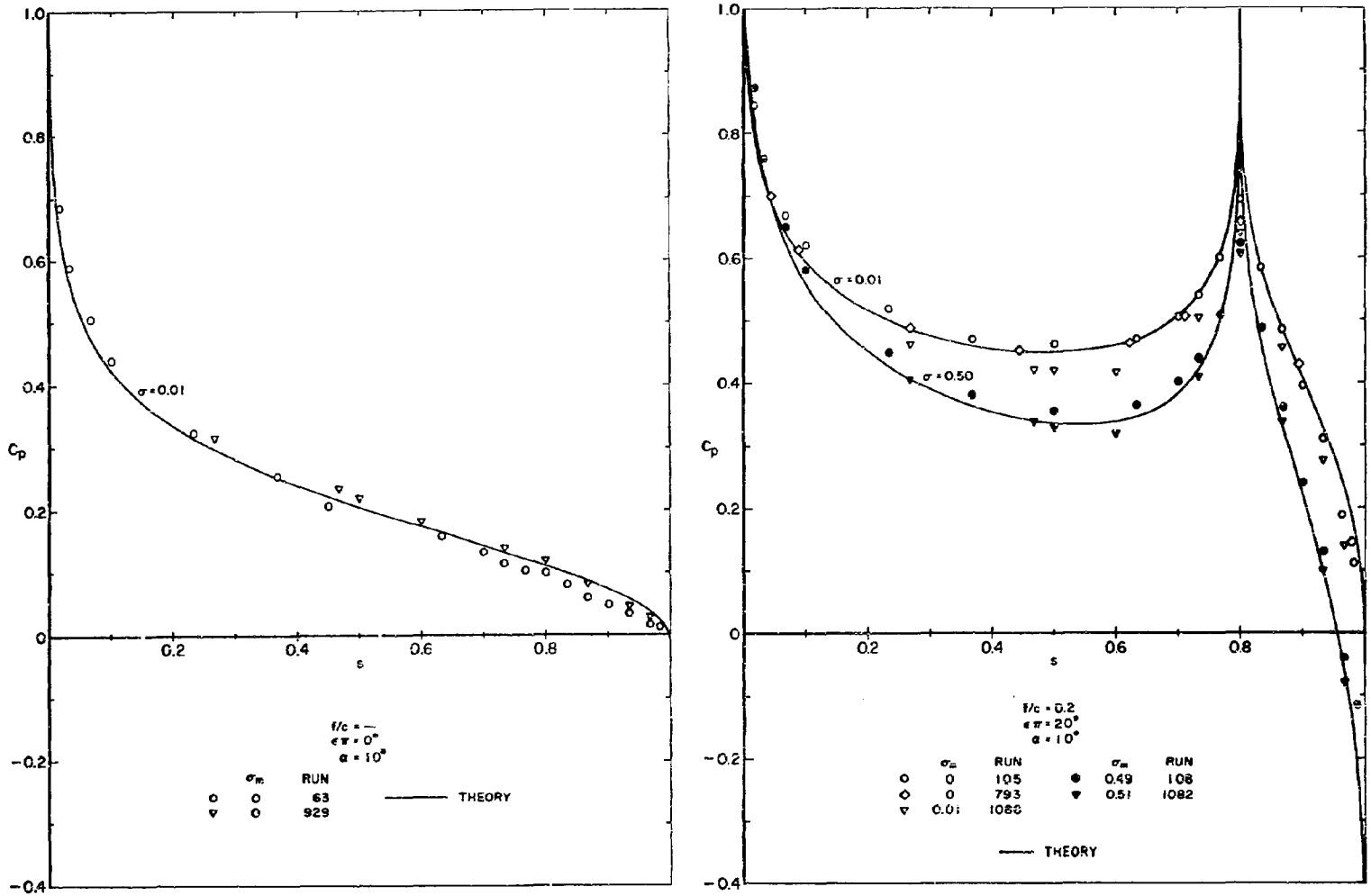

Fig. 9 The pressure distributions for a flapped flat plate with f/c = 0.2, $\alpha = 10^{\circ}$ and $\epsilon\pi = 0^{\circ}$, 20°, 40° and 60° compared with the experimental data of Meijer.

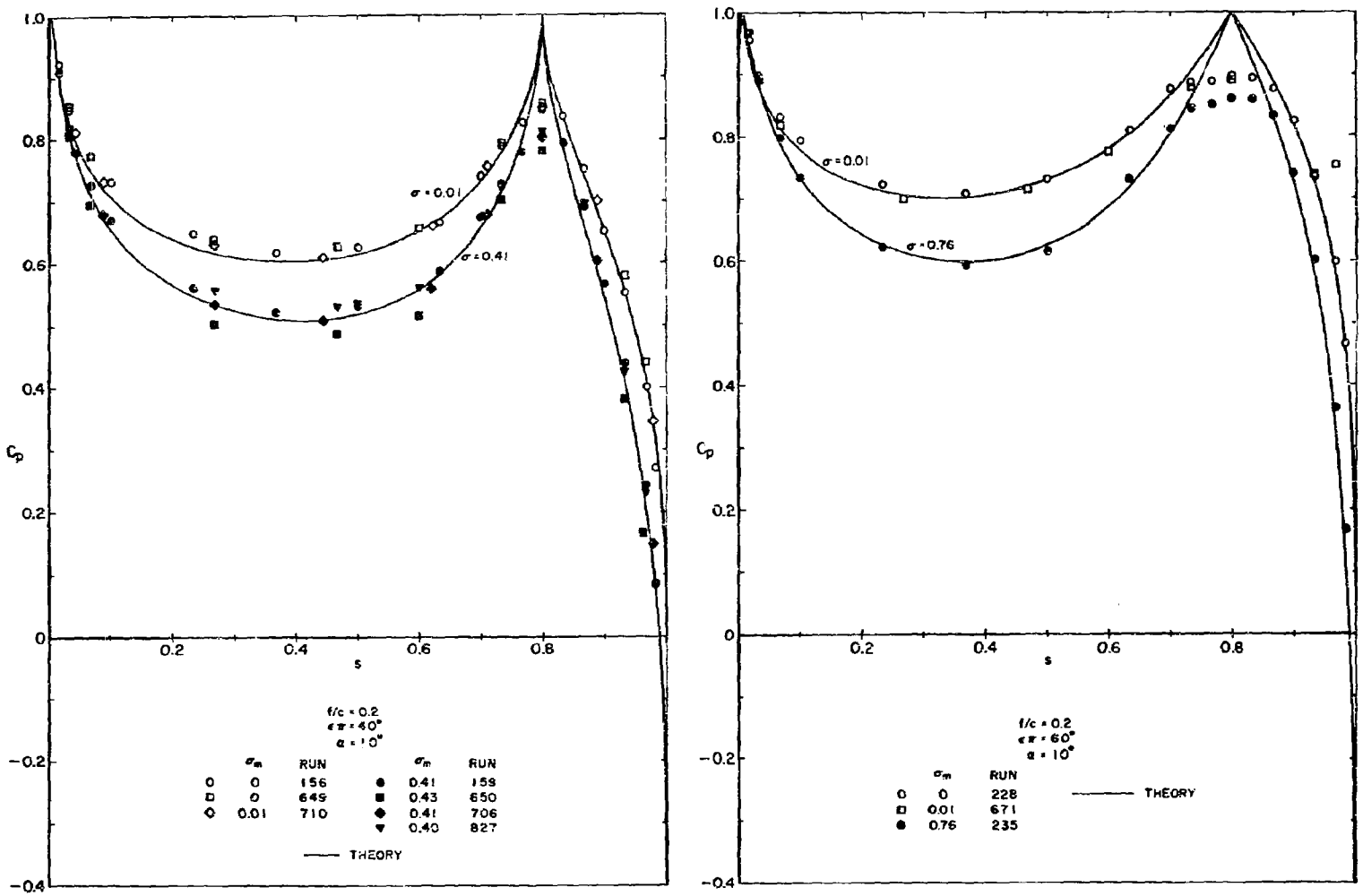

Fig. 9 Continued

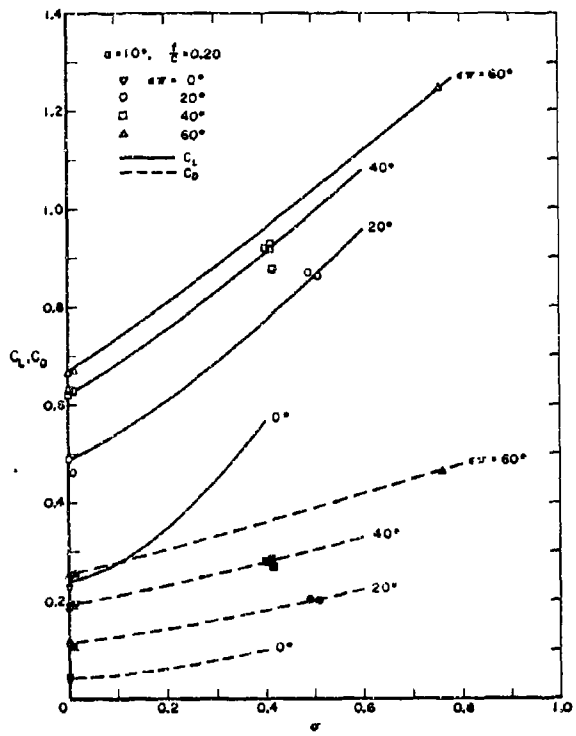

Fig. 10 The comparison between theory and experiment for C_L and C_D. The open symbols indicate the values of C_L and the solid symbols those of C_D obtained by integrating curves through the experimental data in Fig. 9.

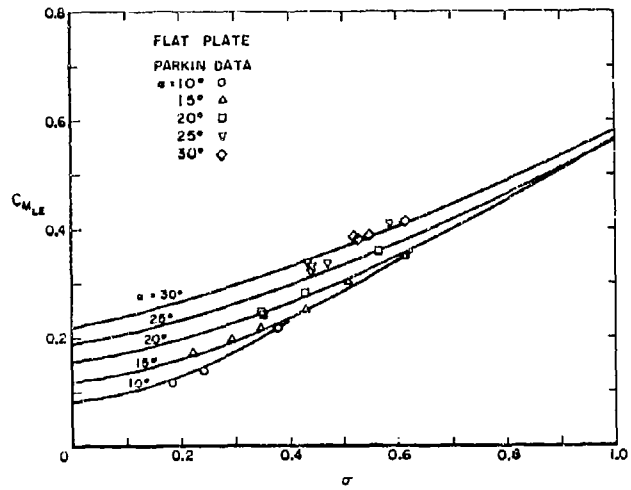

Fig. 11 The comparison between theory and experiment of $C_{M_{LE}}$ for a flat plate. The σ's in Parkin's experimental data are obtained from measured cavity pressures.

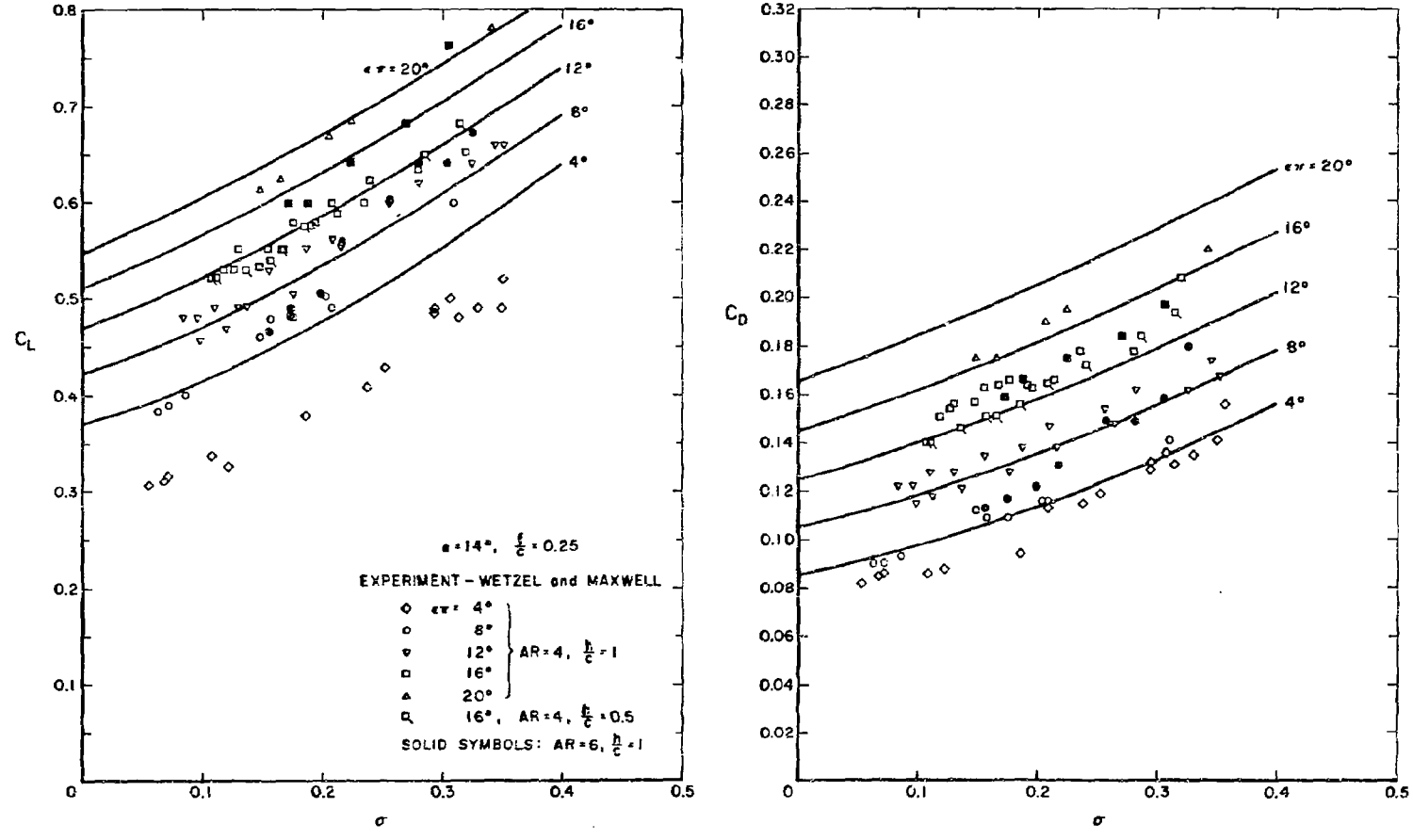

Fig. 12 The comparison between theory and experiment of C_L and C_D for a flapped flat plate with f/c = 0.25 and α = 14°.

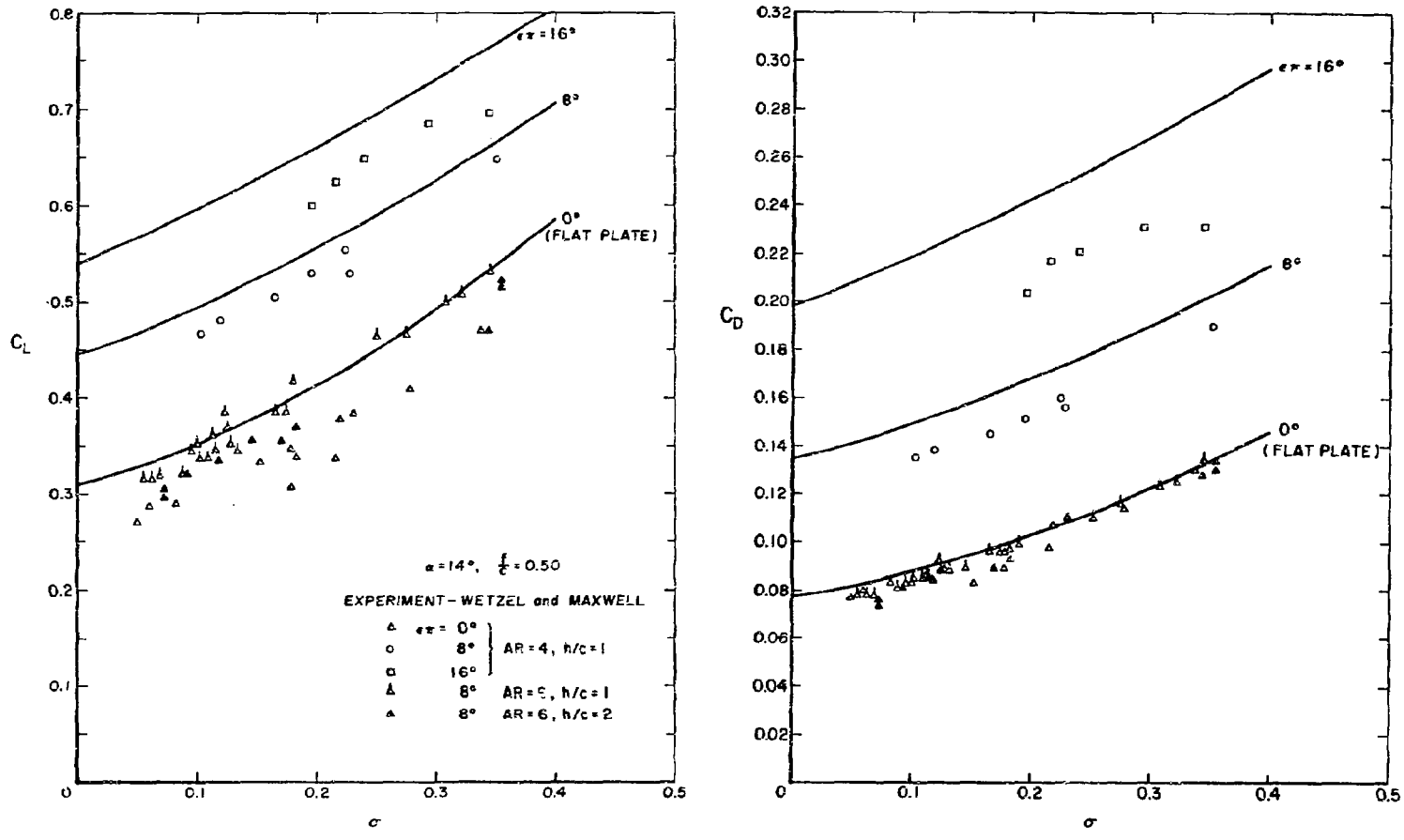

Fig. 13 The comparison between theory and experiment of C_L and C_D for a flapped flat plate with f/c = 0.5 and $\alpha = 14^\circ$.

Unclassified

Security Classification

DOCUMENT CONTROL DATA - R&D

(Security classification of title, body of abstract and indexing annotation must be entered when the overall report is classified)

1. ORIGINATING ACTIVITY (Corporate author)	2a. REPORT SECURITY CLASSIFICATION
California Institute of Technology	Unclassified
	2b. GROUP

3. REPORT TITLE

Evaluation of Pressure Distribution on a Cavitating Hydrofoil with Flap

4. DESCRIPTIVE NOTES (Type of report and inclusive dates)

Final

5. AUTHOR(S) (Last name, first name, initial)

Harrison, Zora L. and Wang, Duen-pao

6. REPORT DATE	7a. TOTAL NO. OF PAGES	7b. NO. OF REFS
September 1965	51	11

8a. CONTRACT OR GRANT NO.	9a. ORIGINATOR'S REPORT NUMBER(S)
Nonr-220(52)	
b. PROJECT NO.	E-133.1
c.	9b. OTHER REPORT NO(S) (Any other numbers that may be assigned this report)
d.	

10. AVAILABILITY/LIMITATION NOTICES

"Qualified requesters may obtain copies of this report from DDC."

11. SUPPLEMENTARY NOTES	12. SPONSORING MILITARY ACTIVITY
	Department of the Navy Office of Naval Research

13. ABSTRACT

A general method is established to calculate the pressure distribution and the moment of force for a two-dimensional, supercavitating hydrofoil with a flap. The wake flow model is adopted to describe the configuration of the flow field. Some numerical results for a supercavitating flat plate with a flap are compared with the corresponding experimental data.

DD FORM 1 JAN 64 1473 0101-807-6800

Unclassified

Security Classification

Unclassified

Security Classification

14. KEY WORDS	LINK A		LINK B		LINK C	
	ROLE	WT	ROLE	WT	ROLE	WT
1. Cavity Flow 2. Hydrofoil with a Flap 3. Pressure Distribution and Moment of Force						

INSTRUCTIONS

1. ORIGINATING ACTIVITY: Enter the name and address of the contractor, subcontractor, grantee, Department of Defense activity or other organization *(corporate author)* issuing the report.

2a. REPORT SECURITY CLASSIFICATION: Enter the overall security classification of the report. Indicate whether "Restricted Data" is included. Marking is to be in accordance with appropriate security regulations.

2b. GROUP: Automatic downgrading is specified in DoD Directive 5200.10 and Armed Forces Industrial Manual. Enter the group number. Also, when applicable, show that optional markings have been used for Group 3 and Group 4 as authorized.

3. REPORT TITLE: Enter the complete report title in all capital letters. Titles in all cases should be unclassified. If a meaningful title cannot be selected without classification, show title classification in all capitals in parenthesis immediately following the title.

4. DESCRIPTIVE NOTES: If appropriate, enter the type of report, e.g., interim, progress, summary, annual, or final. Give the inclusive dates when a specific reporting period is covered.

5. AUTHOR(S): Enter the name(s) of author(s) as shown on or in the report. Enter last name, first name, middle initial. If military, show rank and branch of service. The name of the principal author is an absolute minimum requirement.

6. REPORT DATE: Enter the date of the report as day, month, year, or month, year. If more than one date appears on the report, use date of publication.

7a. TOTAL NUMBER OF PAGES: The total page count should follow normal pagination procedures, i.e., enter the number of pages containing information.

7b. NUMBER OF REFERENCES: Enter the total number of references cited in the report.

8a. CONTRACT OR GRANT NUMBER: If appropriate, enter the applicable number of the contract or grant under which the report was written.

8b, 8c, & 8d. PROJECT NUMBER: Enter the appropriate military department identification, such as project number, subproject number, system numbers, task number, etc.

9a. ORIGINATOR'S REPORT NUMBER(S): Enter the official report number by which the document will be identified and controlled by the originating activity. This number must be unique to this report.

9b. OTHER REPORT NUMBER(S): If the report has been assigned any other report numbers *(either by the originator or by the sponsor)*, also enter this number(s).

10. AVAILABILITY/LIMITATION NOTICES: Enter any limitations on further dissemination of the report, other than those imposed by security classification, using standard statements such as:

(1) "Qualified requesters may obtain copies of this report from DDC."

(2) "Foreign announcement and dissemination of this report by DDC is not authorized."

(3) "U. S. Government agencies may obtain copies of this report directly from DDC. Other qualified DDC users shall request through _____."

(4) "U. S. military agencies may obtain copies of this report directly from DDC. Other qualified users shall request through _____."

(5) "All distribution of this report is controlled. Qualified DDC users shall request through _____."

If the report has been furnished to the Office of Technical Services, Department of Commerce, for sale to the public, indicate this fact and enter the price, if known.

11. SUPPLEMENTARY NOTES: Use for additional explanatory notes.

12. SPONSORING MILITARY ACTIVITY: Enter the name of the departmental project office or laboratory sponsoring *(paying for)* the research and development. Include address.

13. ABSTRACT: Enter an abstract giving a brief and factual summary of the document indicative of the report, even though it may also appear elsewhere in the body of the technical report. If additional space is required, a continuation sheet shall be attached.

It is highly desirable that the abstract of classified reports be unclassified. Each paragraph of the abstract shall end with an indication of the military security classification of the information in the paragraph, represented as *(TS), (S), (C), or (U)*.

There is no limitation on the length of the abstract. However, the suggested length is from 150 to 225 words.

14. KEY WORDS: Key words are technically meaningful terms or short phrases that characterize a report and may be used as index entries for cataloging the report. Key words must be selected so that no security classification is required. Identifiers, such as equipment model designation, trade name, military project code name, geographic location, may be used as key words but will be followed by an indication of technical context. The assignment of links, roles, and weights is optional.

Unclassified

Security Classification